DESIGN AND ANALYSIS OF ELECTRONIC MEASUREMENT CIRCUITS OF INVASIVE ELECTRICAL CAPACITANCE TOMOGRAPHY IN IDENTIFYING OIL-GAS REGIME FOR CONDUCTING PIPE APPLICATION

HAZIQ SYAKIR BIN HAMZAH

B.ENG. (HONS.) ELECTRICAL ENGINEERING (ELECTRONICS)

UNIVERSITI MALAYSIA PAHANG

UNIVERSITI MALAYSIA PAHANG

DECLARATION OF THESIS AND COPYRIGHT

Author's Full Name   : HAZIQ SYAKIR BIN HAMZAH

Date of Birth   : 11 MAY 1997

Title   : DESIGN AND ANALYSIS OF ELECTRONIC MEASUREMENT CIRCUITS OF INVASIVE ELECTRICAL CAPACITANCE TOMOGRAPHY IN IDENTIFYING OIL-GAS REGIME FOR CONDUCTING PIPE APPLICATION

Academic Session   : SEMESTER 2 2021/2022

I declare that this thesis is classified as:

☐ CONFIDENTIAL (Contains confidential information under the Official Secret Act 1997)*

☐ RESTRICTED (Contains restricted information as specified by the organization where research was done)*

☑ OPEN ACCESS I agree that my thesis to be published as online open access (Full Text)

I acknowledge that Universiti Malaysia Pahang reserves the following rights:

1. The Thesis is the Property of Universiti Malaysia Pahang
2. The Library of Universiti Malaysia Pahang has the right to make copies of the thesis for the purpose of research only.
3. The Library has the right to make copies of the thesis for academic exchange.

Certified by:

_____
(Student's Signature)

970511-01-6029
_____
New IC/Passport Number
Date:

_____
(Supervisor's Signature)

_____
Name of Supervisor
Date: 25/6/22

TS. DR. YASMIN BINTI ABDUL WAHAB
PENSYARAH KANAN
FAKULTI TEKNOLOGI KEJURUTERAAN ELEKTRIK DAN ELEKTRONIK
UNIVERSITI MALAYSIA PAHANG
26600 PEKAN, PAHANG

NOTE: * If the thesis is CONFIDENTIAL or RESTRICTED, please attach a thesis declaration letter.

THESIS DECLARATION LETTER (OPTIONAL)

Librarian,
Perpustakaan Universiti Malaysia Pahang,
Universiti Malaysia Pahang,
Lebuhraya Tun Razak,
26300, Gambang, Kuantan.

Dear Sir,

CLASSIFICATION OF THESIS AS RESTRICTED

Please be informed that the following thesis is classified as RESTRICTED for a period of three (3) years from the date of this letter. The reasons for this classification are as listed below.

      Author's Name
      Thesis Title

      Reasons   (i)

                     (ii)

                     (iii)

Thank you.

Yours faithfully,

_____
    (Supervisor's Signature)

Date:

Stamp:

Note: This letter should be written by the supervisor, addressed to the Librarian, *Perpustakaan Universiti Malaysia Pahang* with its copy attached to the thesis.

SUPERVISOR'S DECLARATION

I hereby declare that I have checked this thesis and, in my opinion, this thesis is adequate in terms of scope and quality for the award of the B.Eng. (Hons.) Electrical Engineering (Electronics)

_____

(Supervisor's Signature)

Full Name : TS. DR. YASMIN BINTI ABDUL WAHAB
             PENSYARAH KANAN
Position : FAKULTI TEKNOLOGI KEJURUTERAAN ELEKTRIK DAN ELEKTRONIK
             UNIVERSITI MALAYSIA PAHANG
Date   : 26600 PEKAN, PAHANG   25/6/22

_____

(Co-supervisor's Signature)

Full Name :

Position :

Date   :

STUDENT'S DECLARATION

I hereby declare that the work in this thesis is based on my original work except for quotations and citations which have been duly acknowledged. I also declare that it has not been previously or concurrently submitted for any other degree at Universiti Malaysia Pahang or any other institutions.

_____

(Student's Signature)

Full Name   : HAZIQ SYAKIR BIN HAMZAH

ID Number   : EA18072

Date   : 23/6/2022

DESIGN AND ANALYSIS OF ELECTRONIC MEASUREMENT CIRCUITS OF
INVASIVE ELECTRICAL CAPACITANCE TOMOGRAPHY IN IDENTIFYING
OIL-GAS REGIME FOR CONDUCTING PIPE APPLICATION

HAZIQ SYAKIR BIN HAMZAH

Thesis submitted in fulfillment of the requirements

For the award of the B.Eng. (Hons.) Electrical Engineering (Electronics)

College of Engineering

UNIVERSITI MALAYSIA PAHANG

JUNE 2022

ACKNOWLEDGEMENTS

ABSTRAK

Projek ini adalah berkenaan kaedah tomografi kemuatan elektrik (ECT) secara invasif bagi penentuan perubahan nilai kumuatan yang disebabkan oleh perubahan taburan kemiringan bahan dielektrik yang berbeza seperti minyak dan air di dalam saluran paip. Dalam projek ini, sebanyak 8 elektrod telah digunakan. Peranti direka untuk mendapatkan taburan potensi elektrik antara setiap elektrod. Litar untuk memancarkan nilai voltan di saluran pemancar dan litar penguat di bahagian penerima elektrod juga telah dibangunkan. Beberapa perbezaan kedudukan, saiz dan lokasi sebagai bahan ujikaji dalam medium minyak telah diuji dalam projek ini. Prestasi peranti juga telah dianalisis dan data juga telah dikumpulkan. Kaedah algoritma Unjuran Belakang Linear (LBP) melalui perisian COMSOL dan MATLAB telah digunakan dalam projek ini. Tomogram yang telah diperolehi telah dibandingkan dengan menggunakan indeks MSSIM. Ianya bertujuan untuk menentukan ketepatan imej yang diperolehi. Hasilnya, imej tomogram bagi setiap keadaan diuji kemudiannya diperhatikan dan dianalisa. Saiz minimum bahan uji kaji yang dapat dikesan oleh projek ini ialah pada diameter 33mm, ia menunjukkan indeks MSSIM yang lebih tinggi berbanding uji kaji 20mm dan 25mm dan tomogram yang dihasilkan oleh uji kaji 33mm juga mempunyai kualiti gambar yang lebih baik. Ringkasnya, pendekatan invasive untuk ECT dilihat boleh digunakan untuk aplikasi minyak-gas dalam paip keluli.

ABSTRACT

This project is to investigate the changes of capacitance value due to the changes of permittivity distribution of different dielectric materials such as water and oil in conducting pipeline using invasive approach of electrical capacitance tomography (ECT). In this project, 8 electrodes of ECT system are developed. Also, the signal generator circuit at the transmitter channel and the amplifier circuit at the receiver were developed. The sensor jig is developed in order to obtain the electrical potential distribution between electrode. A several position, sizes and multiple obstacles as obstacle in oil medium were tested in this paper. The sensor performance inside the sensor jig was analyzed and the data was collected. The data was then used to reconstruct image using the Linear Back Projection Method through COMSOL and MATLAB software. The tomogram was obtained and compared using the MSSIM index to determine the accuracy of the image created. The minimum size that can detect is 33mm in diameter, whereby it shows the higher MSSIM index if compared to the 20mm and 25mm obstacles. Also, the tomogram created by the 33mm obstacle had a better-quality image. In short, the invasive approach for ECT is seen possible to be applied for oil-gas application in steel pipe.

TABLE OF CONTENT

LIST OF TABLES

LIST OF FIGURES

LIST OF SYMBOLS

C	Capacitance
εr	Relative permittivity
εo	Permittivity of free space
A	Area of plate
d	Distance between two plates
E	Electric field
Ei	Electric field intensity
Ed	Electric field with dielectric
φ	Electric field potential distribution within the sensor
ρv	Volume charge density
D	Electric flux density
$Mi,j(x, y)$	Normalizing sensitivity map
Si,j	Signal loss amplitude of receiver
$PLBPnorm$	Conductivity distribution
ε_h	High relative permittivity
ε_l	Low relative permittivity
$\mu(k)$	Ratio of maximum area to kth area
C_{ij}^h and C_{ij}^l	Capacitance of electrode pair at different permittivity, l and h

LIST OF ABBREVIATIONS

ECT	Electrical capacitance tomography
EIT	Electrical impedance tomography
LBP	Linear back projection
MSSIM	Multi scale structural similarity

CHAPTER 1

INTRODUCTION

1.1 Project Background

1.1.1 Overview Of Tomography

Tomography is a technique for creating a three-dimensional image of a solid object's internal structures (such as the human body or the earth) by observing and recording differences in the effects of waves of energy impinging on those structures.

Tomography is used in many fields whether for education or industry proposes. Tomography is commonly found and used in medical field with widely applied the "Computed Tomography" or CT scan. It is a diagnostic imaging procedure whereby the X-rays and computer technology are used to create images of the internal part of the body. It can display comprehensive views of the bones, muscles, fat, organs, and blood arteries in any section of the body[1].

The benefits that industry uses the process tomography such as in the oil industry are to improve the product quality, reduced product development time and reduced inspection cost. The idea for tomography is to install a number of sensors inside the pipe vessel to be imaged[2]. The result of the measurement signal from the sensor is amplified, filtered, and processed in the computer using a specific image reconstruction technique to create a cross-sectional image.

1.1.2 Importance of Study

Electrical Capacitance Tomography (ECT) is a preferred process tomography technique because it is a promising method for imaging multiphase regimes of a chemical processes. It uses external capacitance sensors to assess the examined material's internal permittivity distribution, allowing it to identify various materials based on the electrical

permittivity[3]. Furthermore, ECT provides non-invasive measuring with high-speed capabilities and great accuracy. ECT has been effectively used in a variety of industrial applications involving multiphase flows.

ECT sensor consisting of numerous electrodes, typically 6, 8, 12 or 16 that are typically installed in circular conducting pipe or insulated pipe around the external or internal periphery[3]. ECT study is currently based on the insulation wall vessel and pipelines at present [4][5][6]. However, most industry uses the steel pipeline and vessel. Therefore, this project focused on the ECT system for steel pipe application based on an invasive approach. It uses insulator pad between electrode to avoid a grounding effect.

1.2   Problem Statement

The current research on ECT system only apply a non-invasive and mostly the material used is non-conducting pipe. Most of them uses acrylic or Perspex pipe. Most of the medium used in the industry is a nonconductive medium so that the electrical signal can be transmitted and received eventually. For an oil and gas industry, it mostly uses a steel pipe[7]. Therefore, this project proposed an ECT system that could detect the condition of oil and gas in steel pipes using an invasive approach. It is due to the oil and gas regimes in steel pipe application cannot be applied using non-invasive approach if the ECT system is implemented.

1.3   Objectives

The objectives of this project comprise of the following:

i.   To design a suitable electrical measurement circuit of invasive ECT system including its signal generator and conditioning signal circuits.

ii.   To develop a sensor jig of ECT for oil gas identification in steel pipe using invasive technique.

iii.   To analyse the sensor reading performance invasive of ECT system considering locations, of the different shapes and oil sizes gas regimes

1.4 Scopes of Project

The scopes of this project are:

i.   Sensor is limited for 8 electrodes.

ii.   The material of the pipe, electrodes and insulator are steel, copper and flexible FR4 respectively.

iii.   The inner of diameter for the pipe is 75mm.

1.5 Thesis Organisations

Introduction, literature review, methodology, findings, discussion, and conclusion are all important parts of this thesis. The purpose of the introduction chapter is to provide a brief overview of tomography, the necessity of the study, the problem statement, and the project's objectives and scopes. In addition, chapter two reviews the current research in process tomography mainly in electrical capacitance tomography information. Besides, the chapter about methodology explains about the software used to design the circuit, COMSOL Multiphysics in getting the sensitivity map, and the MATLAB software for image reconstruction of the region of interest. For chapter four, the result and analysis for the image reconstruction from MATLAB software was shown. Finally, the conclusion chapter is the most significant chapter since it summarises all of the project work for this invasive electrical capacitance tomography approach, as well as the problem faced during the project and future recommendation for future reference.

CHAPTER 2

LITERATURE REVIEW

2.1 Process Tomography

2.1.1 Introduction

Tomography technology has been around for since 1950s which started the development of tomographic instrumentation. It has led to international availability of body scanners nowadays [4]. Tomography technology comprises of the acquirement of measurement signals from the electrodes positioned on the periphery of an object, such as process vessel or pipeline[8].

The process of tomography should be containing the hardware system consisting of sensor and measurement circuits, software for imaging reconstruction and a display unit to present the image created. The sensor will then measure the object present. After undergoing the image reconstruction algorithm process, the information and distribution of components will be reconstructed in the form of a cross-sectional image that can be viewed on a computer. For example, in this project, the information and distribution of oil-gas regime in the steel pipe was revealed[7].

There are various kinds of techniques or methods of tomographic measurement used in industrial process such Electrical Resistance Tomography, Optical Tomography, Electrical Capacitance Tomography, Ultrasound or Ultrasonic Tomography. The technique mainly consists of 4 main parts, the sensing system, electronic measurement system, data acquisition system, and the result display [9].

2.1.2 Electrical Impedance tomography

Electrical impedance tomography is also called as potential tomograph. It is a non –
invasive method which is able to determine the electrical conductivity of a medium by
making voltage and current measurements at the boundaries of the object [4]. EIT is the
most recent and sophisticated impedance sensing system used for electrically conducting
materials. It is used for clinicals applications [4]. It measures the changes in both
resistance and the reactive components from a multi electrode sensor of a system or
materials.

EIT is being applied to industrial process environment where the process uses
conducting fluid to carry immiscible fluids and solids, which contain different bulk
conductivity[4]. EIT is relatively low cost in comparison with other tomographic
methods. It is also very compact due to absence of large transducer and ease of integration
of a purely electronic system[3]. And it is safe to be used in comparison to X Ray
methods. The shortcoming of EIT is that it cannot be used in pneumatic conveying which
comprises of large electrically non- conducting solids [4].

2.1.3 Electrical Resistance Tomography

Electrical capacitance tomography is used to determine electrical conductivity by
measuring voltage around the vessel's perimeter[4]. ERT involves the acquisition of
measurement signals. It is mainly used for the measurement of gas liquid and other mixed
signals.

Measurement of electrical resistance via four probes is widely used in a range of
application such as in Ref. [4]. For example, in biomedical and measurement, resistance
tomography uses a circular array electrode for its measurement. This is achieved by using
four electrodes around a body for measurement purposed[8].

2.1.4 Ultrasonic tomography

Ultrasonic sensor have been successfully applied in flow measurement, it is a non-
destructive testing method and widely used in medical imaging[4]. Ultrasonic sensor
system is measured upon the interaction between the incident of ultrasonic waves and the
object to be imaged. For instance, incident waves may be reflected from boundaries; the

reflections may be detected, and the data processed to determine the boundary's location. Therefore, ultrasonic sensors are only useful in processes where large interactions occur, and when such interactions generate a higher level of measurable information than is available in conventional transduction techniques[10]. In ultrasonic tomography, the required equipment's are ultrasonic generator, ultrasonic transducers to transmit and receive ultrasonic waves and a computerized image processing system. This type of tomography is mostly higher than other tomography methods due to the cost of transmitter and receiver is high. Besides, ultrasound transmitter is driven by voltage of hundreds of volts which makes an intrinsically safe system hard to develop[11].

2.2   Electrical Capacitance Tomography

Electrical Capacitance tomography is a system which can be used for imaging industrial multi component process involving non-conducting flids in pipelines[11]. It is a technique used to visualize the distribution of two differing dielectric components. It measures variations on the dielectric properties of the materials inside the vessel[12]. Its basic principle is to measure the changes in capacitance from a multi-electrode sensor, and then reconstruct a permittivity distribution. For example, the image is constructed using the measured capacitance data[4].

The ECT system is developed by installing a number of conducting plates (electrodes) around the periphery of the vessel. When a dielectric material is introduced inside the sensor measuring area, the capacitance variations which occur between combinations of electrodes can be measured[13]. ECT is mainly develop for industrial process, because it will detect the variation of permittivity distribution in the closed region or pipe vessel [9]. The images will be reconstructed based on the signal obtained at each of the receivers of the capacitors electrodes[9].

2.3   Principle of Electrical Capacitance Tomography

The basic principle of an ECT system is to record capacitance changes from a multi-electrode sensor and then reconstruct a permittivity distribution using that data. The sensors in these applications are generally made up of two electrode plates and a capacitance sensor[4][11]. Figure 2.1 shows the ECT system topology. It generally

consists of signal generator circuit, signal conditioning circuit, control unit and computer for image reconstruction part.

The sensors for tomographic imaging should allow for numerous and localised measurements across the study area, according to the requirements. To produce a "body scan" of the imaging volume, many electrodes should be positioned around the region's perimeter and the capacitance between all the combination pairs of electrodes should be determined.

The initial electrode (named electrode 1), which becomes the excitation electrode, begins a complete cycle for an ECT system measurement[14]. All other electrodes that function as receivers get the capacitor value that corresponds to the dielectric in between when the source electrode (also known as the source electrode) is supplied with a sine wave. Capacitances between electrodes 1 and 2, 1 and 3, 1 and 4, and 1 and the last electrode, for example, are all measured in sequence. Detecting electrodes are electrodes other than electrode 1 that are at the virtual earth potential imposed by the transducer during this measurement period. After that, electrode 2 will operate as the source electrode, with the remaining electrodes acting as detecting electrodes[4]. The processes continue until each electrode has become the source electrode, at which point the cycle is complete. The projected guards and the system screen are constantly kept at earth potential.
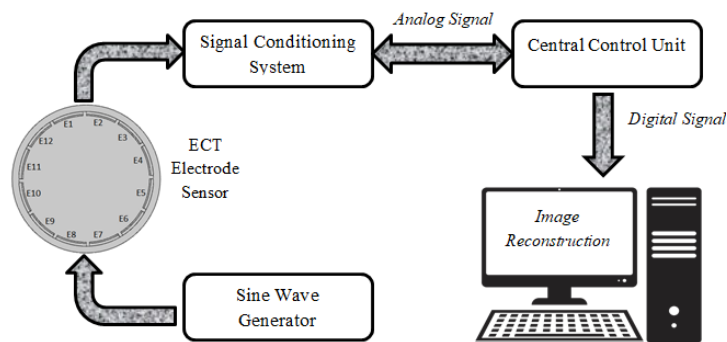
Figure 2.1 ECT system topology[4]

2.3.1   Capacitance

A capacitance is basically consisting of two conducting surfaces separated by a layer of an insulating medium called dielectric. The property of capacitor to store electricity is called capacitance[15]. The quantity of charge required to create a unit potential

19

difference between its plates is known as capacitance. Capacitor consists of two conductors; common capacitor has same size of conductor but different charge[16][17].
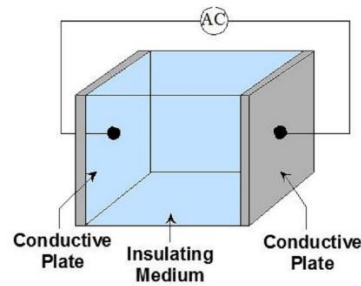

Figure 2.2 Two conductor common capacitor with equal size but different charge on the conductors

A two-conductor capacitor's capacitance is defined as the ratio of the magnitude of charge on one conductor to the magnitude of the potential difference between two plates of conductors (A and B) as shown in Figure 2.2, with dielectric material between the plates. The formula for the capacitance is [4].

$$C = \frac{|Q|}{|V_{AB}|} \qquad 2.1$$

Where V_{AB} is the potential difference between any point on conductor A, B and Q is charge in coulomb. The unit for capacitance is Farad (F). The derivation between electric field intensity, E and electric flux density, D are shown in in Equation 2.2 and 2.3.

$$E = \frac{V}{d} \qquad 2.2$$

$$D = \frac{Q}{A} \qquad 2.3$$

If the Equation 2.2 is substitute in Equation 2.3, thus:

$$\therefore \frac{Q}{V} = \varepsilon \frac{A}{d} \qquad 2.4$$

Finally, the relationship between capacitance and permittivity is

$$C = \frac{\varepsilon_0 \varepsilon_r A}{d} \qquad 2.5$$

where,

C = capacitance (F)

ε_o = permittivity of free space = $8.85 \times 10-12 Fm-1$

ε_r = relative permittivity of the dielectric, also simply referred to as permittivity

A = area of the plate

d = the distance between those plates

The ε_o and ε_r represent the global average of the material dielectric property throughout the sensor's whole sensing volume, also known as electrical permittivity. By measuring the capacitance, we are essentially measuring the dielectric constant [15][12]. if the area of the plate and the distance between them are known. The sensing area of the electrodes can be enlarged to enhance the signal-to-noise ratio (SNR) of the readings.[4].

2.3.2 Dielectric

When a dielectric component is placed in an electrical field (between two plates), it induces a field Ei on its surface. As a result, the electric field between the two conductors is transformed into

$$E_d = E + E_i \qquad\qquad 2.6$$

Where,

E = Electric field
Ei = Electric field induce
Ed = Electric field with dielectric

The capacitor will increase with the factor of $k = \dfrac{\varepsilon}{\varepsilon_d}$, when a dielectric component exists between the conductors [1]. Table 2.1 shows the dielectric constant for several types of material.

Table 2.1 List of dielectric constant[13]

Material	Dielectric constant
Vacuum	1.0
Air	1.0006
Polythene	.2.0-2.5
Nylon	3.4
Paper	3.7
Quartz	3.78
Insulating Oil	3.0-4.0
Glass	5.0-10.0
Porcelain	6.0-7.0
Distilled water	80.0

2.3.3 Poisson Equation of ECT

An ECT system is made up of a number of electrodes that surrounding a pipe or vessel. The number of independently measured capacitances matches the number of independently measured electrode pairs[18]. The capacitances measured are required to reconstruct the permittivity distribution within the vessel. According to the Poisson equation, the electric potential is influenced by the permittivity distribution[19].

$$\nabla \cdot (\varepsilon(x,y)\nabla\emptyset(x,y)) \ = \ -\rho(x,y) \qquad\qquad 2.7$$

where,

$\varepsilon(x, y)$ is the electrical permittivity distribution,

$\emptyset(x, y)$ is the electrical potential distribution

$\rho(x, y)$ is the charge distribution

Noted that, the Poisson equation is a linear partial differential equation in terms of $\emptyset(x,y)$. The non-linearity in ECT refers to the nonlinear dependency of $\emptyset(x,y)$ on $\varepsilon(x,y)$[20].

2.4 Invasive and Non-Invasive technique

Invasive means the sensor is placed into the vessel, whereas non-invasive means the sensor is not inserted into the vessel. Non-destructive, non-intrusive, and non-invasive qualities should all be included in a good tomography sensor.

2.4.1 Invasive Technique

Another different arrangement is to fit the electrodes inside the vessel as shown in Figure 2.3. The case of a metal walled vessel, this requires the use of an insulated liner to support the electrodes, which is also placed within the vessel[1]. This type of sensor has the highest accuracy. In this Figure 2.3, it requires some form of insulated linear supporting the electrodes. Although it is more difficult to design and build this sort of sensor from a mechanical aspect, sensors with electrodes inside the vessel do not have the non-linearity issues that sensors with electrodes outside the vessel do[9].
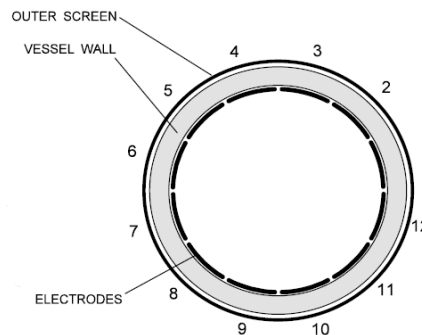

Figure 2.3 ECT with internal electrode[4]

2.4.2 Non-Invasive Technique

From a construction aspect, the simplest design consists of a nonconducting piece of pipe contained by an array of evenly spaced capacitance electrodes with an overall earthed screen. The sensor of this type is shown in Figure 2.4. Electrodes that are set up in a non-invasive manner will keep the sensor from coming into close contact with the fluid, and hence it can prevent contamination. This type of sensor has lower accuracy because of the presence of the sensor wall. ECT using a non-invasive technique, on the other hand, might exhibit significant non-linearity in their reaction to dielectric materials inserted inside the sensor[13].
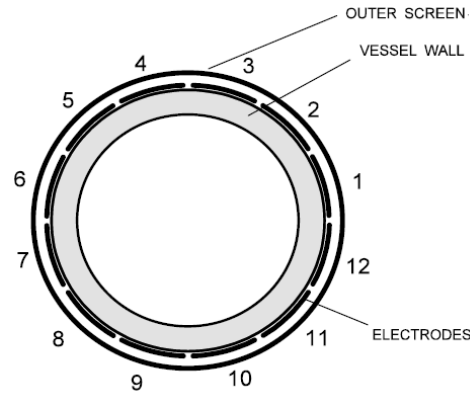
Figure 2.4 ECT with external electrode[4]

2.5   Linear Back Projection Algorithm

After all of the sensor data has been collected, the data will be subjected to an image reconstruction procedure. Non-iterative and iterative image reconstruction techniques are the two types of image reconstruction algorithms. To extract measurable data from cross-sectional images of a multiphase pipe flow, high-quality capacitance tomography data reconstruction is required[21][22].

Linear back projection is the example for non-iterative algorithm. It is used in this project. The simplest version of this algorithm assumes that sensitivity remains constant within the sensitivity range[23]. The LBP algorithm offers the advantage of a simpler computational method and the ability to make images faster.

Each sensitivity matrix is multiplied by the comparable sensor reading as shown in Equation 2.8. It was done to rebuild the picture utilising an LBP algorithm approach. To increase the data density of the projection, the back projected data values are smeared across the unknown density function (image) and overlapped. As a result, one of the most significant drawbacks of the LBP algorithm is that it produces a blurred image, often known as the smearing effect [21].

$$G_{LBP}(x, y) = \sum_{i=1}^{T} \sum_{j=1}^{R} J_{ij}(x, y) \times L_{i,j}$$

2.8

$P_{LBP}(x, y)$ is the conductivity distribution obtained using LBP algorithm or the concentration profile and N is the number of electrodes[4]. The tomogram generated by

24

the LBP method was normalised from 0 to 1 for simple comparison and the normalize sensor loss in this project as shown in Equation 2.9.

$$J_{ij} = \frac{S_{ij}^{inc} - S_{ij}^{tot}}{S_{ij}^{inc}}$$

2.9

Where,

T	= The number of excitation electrodes
R	= The number of measuring electrodes
L_{ji}	= Sensitivity map at each I and j
$J_{ij}(x, y)$	= Corresponding signal loss / sensor loss
S_{ij}^{tot}	= The electrical potential measured when there is obstacle in Sensor Jig
S_{ij}^{inc}	= The electric potential measured when there is no obstacle in Sensor Jig

2.6   Summary

In this chapter, several types of tomography sensors have been discussed. Based on the information above, it can be stated that each type of tomography sensor has its own set of advantages and disadvantages. Different types of tomography sensors are suitable for imaging different sorts of fields. The ECT has the benefit of being able to measure variations in the dielectric properties of materials inside a pipe, making it a viable imaging technology for industrial applications. Besides, the detail about linear back projection (LBP) algorithm was also explained.

CHAPTER 3

METHODOLOGY

3.1   Introduction

This chapter is to concentrate on the design and develop a sensor jig of electrical capacitance tomography for oil and gas identification in steel pipe. The electrodes are placed using invasive technique, which the electrode is put inside the steel pipe. Figure 3.1 shows the basic measuring flows system where the ECT sensor consists of twelve electrodes attached equidistantly along the periphery of the conducting pipe vessel. The 8 segmented electrodes are labelled from 1 to 8, the measurement of the electrode's need to take place between electrode one and two, then between one and three until electrode to k, where k is 8 for this system[21]. Then, the ECT system is then measured between electrode two and three and up to two and k are measured. The measurement remains until all the inter electrodes capacitance are measured.
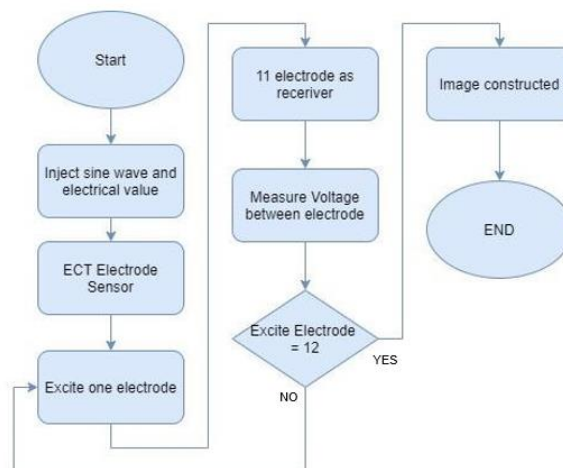
Figure 3.1 Basic flow process of the ECT

An ECT system consists of a set of symmetrically mounted electrodes inside or outside and insulation pipe. This research consists of 8 electrodes, a measurement circuit, control central unit and a control PC. The electrode is built from copper plate and acts as a sensing surface. The capacitance measuring cirucit is also known as signal conditioning circuit. It is uses to collect data and convert the measurement readings to digital. All processes are synchronised and data is sent to a control PC through the central control unit.Then, the obtained data will be saved on the control PC that receives the measurement reading. The gathered data is then used to rebuild pictures from integral measurements and take action to manage the flow in real time.

In this project, the signal conditioning circuit consists of absolute value circuit and low pass filter. Other than that, a high frequency sine wave generator is required as a source to excite the electrode sensor. the absolute value circuit data is converted to digital current using the low pass filter. The digital data will then be transferred to a computer for image reconstruction and analysis. The block diagram of ECT system is depicted in Figure 3.2.
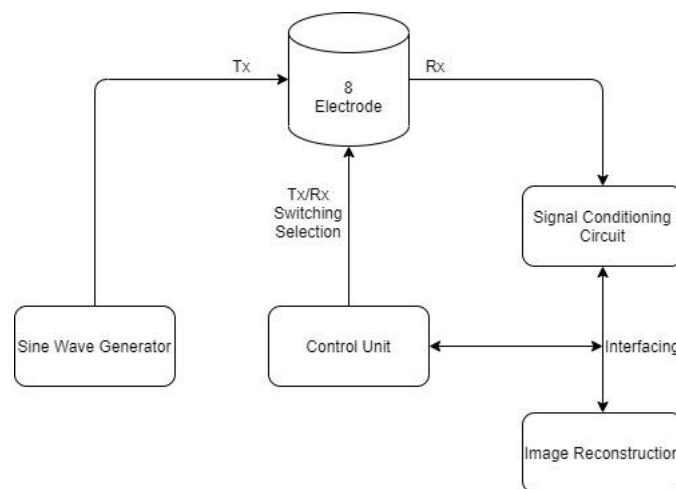

Figure 3.2 Block diagram of ECT system

3.2   Software Tools

In simulating the circuit simulation part, Multisim software had been used to design the signal conditioning circuit and signal generator circuit. NI Multisim is an electrical schematic capture and simulation application that, along with NI Ultiboard, is part of a suite of circuit design programmes. Multisim provides microcontroller simulation as well as integrated import and export functionality for NI Ultiboard, the suite's printed circuit

board designing software. For circuits teaching, electrical schematic design, and SPICE simulation, Multisim is extensively used in academia and industry.

Figure 3.3 NI Multisim Software

In designing the sensor jig, AutoCAD 3D is used d to set up all sensor used and also design the object. AutoCAD aid in the creation, modification, analysis, or optimization of a design. CAD may be used to design curves and figures in two-dimensional (2D) space; or curves, surfaces, and solids in three-dimensional (3D) space. It also been used to determine the dimension of the system.

Figure 3.4 AutoCAD software

3.3   Sensor Jig Design

The first step in developing a sensor jig is by determining the parameter of the pipe and with a certain diameter. For this case, the parameters such as diameter of the pipe and the dimension of the electrode of the drawing geometry are based on the literature review. Then, alteration of the number of electrodes and the insulator pad around the pipeline could be easily built. In this research, some of the parameter is fixed in the sensor jig design as illustrated in Table 3.1. The Sensor Jig coverage is needed to be at least 90% of the area, it is because that the higher the coverage of the sensor jig, the more accurate the data recorded. The sensor height and width were 200mm and 18mm respectively. The sensor front and rear side is shown in Figure 3.5 and Figure 3.6. The coverage of the sensor jig and sensor jig design is shown Figure 3.7 and Figure 3.8.

Table 3.1 List of Parameter

Item	Parameter
Number of electrodes	8
Outer Diameter pipe	76mm
Electrode stretch angel, θ (90% of angle) Thickness of electrode	$\frac{360}{12} = 45° \& \frac{90}{100} \times 45° = 40.5°$ 1mm
Insulator stretch angle, θ (90% of angle) Thickness of insulator	$\frac{360}{12} = 45° \& \frac{90}{100} \times 45° = 40.5°$ 2mm

Figure 3.5 Front side of the sensor and sensing area

Figure 3.6 Rear Side of Sensor
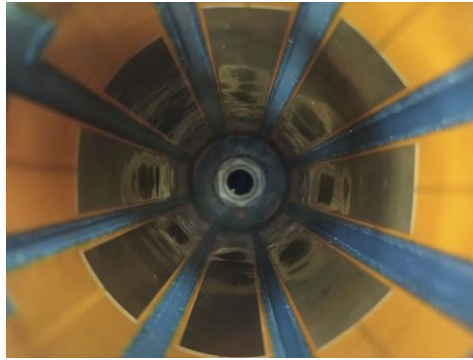
Figure 3.7 Placement of electrode inside sensor jig

Figure 3.8 Sensor Jig design

3.3.1 Physical Sensor Parameter

The physical sensor parameter was determined based on the literature review. This physical sensor parameter was fixed due to the previous studies that uses this parameter. By using the parameter, the result was compared with the previous studies result.

Table 3.2 Physical Sensor Parameter

DOMAIN	PARAMETER	VALUE
Pipe	Outer diameter pipe	76mm
	Inner diameter pipe	74mm
	Thickness of pipe	2mm
	Material	Structural steel
	Relative Permittivity, εr	1
Electrode	Number of electrodes	8
	Stretch angle of electrode	40.5º
	Thickness of electrode	1mm
	Material	Copper
	Relative Permittivity, εr	1
Insulator pad	Number of insulators	8
	Stretch angle of insulator	40.5º
	Thickness of insulator	2mm
	Material	FR4
	Relative Permittivity, εr	4.5
Oil	Relative Permittivity, εr	3.25
Air	Relative Permittivity, εr	1

3.4   Hardware Development

The hardware development of the ECT system was held up by using all the parameters that had been considered. The function generator will supply 7.99Vpp, 150kHz sinusoidal signal and it is connected to an amplifying circuit. The amplifying circuit is consisting of non-inverting circuit that will amplify the signal to 20Vpp, 150kHz. The reason to use the 150kHz is because when the frequency is too high, the signal will change from sine wave to triangular waveform. Hence, it was not achieving the waveform that is required for the ECT system.

After that, the signal was injected into electrode 1, while the other 7 electrodes acted as the receivers. The step will be repeated until all the 8 electrodes become as the excitation source. Then, at the receiving terminal, the signal value will be recorded. To record the signal, it will go to the signal conditioning circuit where the signal from the electrode will be improved. The signal will also be amplified at the signal conditioning circuit. Then, the signal will be observed using the oscilloscope and the electrical potential value is recorded. Finally, the data recorded will be used to construct an image of the tomogram using the MATLAB software. The flow chart of the hardware is shown in Figure 3.9.
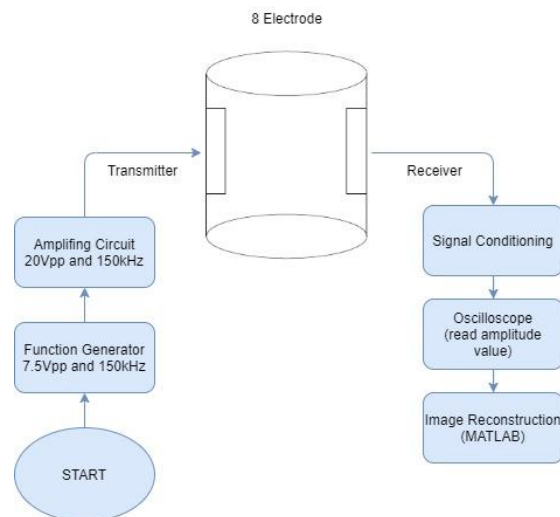

Figure 3.9 Hardware Development

3.4.1   Electronic Measurement Circuit

3.4.1.1   Signal Generator Circuit

A signal generator is an electronic device that generates analogue or digital signals that are both repeating and non-repeating[24]. The signal generator is widely

utilized in troubleshooting, signal tracing, testing, amplifier response modification, and radio and television circuit alignment[4][25].For this project, the non-inverting operational amplifier has been chosen, it is mainly because the of the output voltage is in phase with input voltage. The IC used is the TLE2141IP which support the frequency value used for this circuit. This system input is 7.99 V_{PP} and 150kHz. The output voltage is increased until 20 V_{PP} and 150kHz. Figure 3.10 is the simulation result for the system.
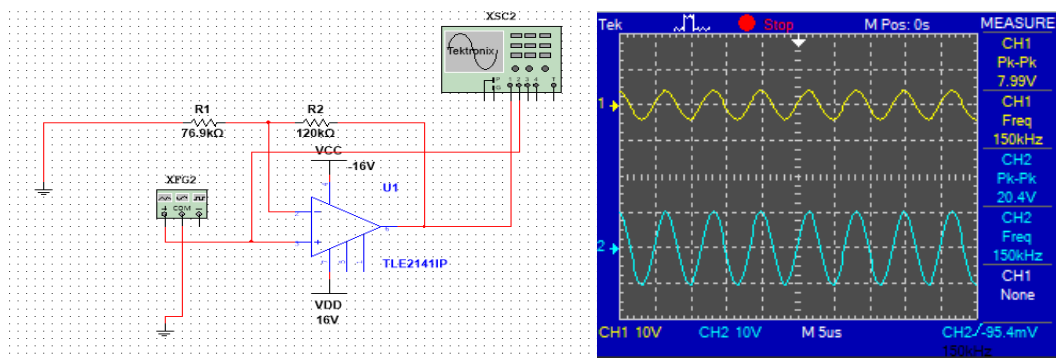
Figure 3.10 Circuit and result for signal generator circuit

3.4.1.2   Signal Conditioning Circuit

Accurate data can only be obtained with a good design in sensing electronics that is able to eliminate noises. An important issue with instrumentation design performance of the circuit is the performance of the circuit's presence of noise[4]. In selecting and designing a capacitance measuring circuit, the stray immune circuit must be selected to satisfy this requirement[25]. Because all of the measurement processes are handled by a separate microcontroller on the circuit, each signal conditioning circuit is distinct and capable of working independently[25].

In this project, the signal conditioning system measures the capacitance produced by the electrode pairs when a 150kHz sine wave voltage with and amplitude of 20Vpp is injected to one of the electrode pairs.

3.4.1.3   Non-Inverting Amplifier and Peak Voltage Detector

The circuit of non-inverting amplifier and peak voltage detector is shown in Figure 3.11. The non-inverting circuit is used to amplify the sensor reading because the value is too small. The signal was amplified using the circuit from 10.4mVpp to 5.24Vpp. The

circuit has also been improved to reduce noise that came from the sensor. A 56kΩ was connected at point 2 to the ground, this was to normalized the frequency of the system since the frequency was unreadable. A capacitor with 1uF was also added to reduce the noise coming from the sensor and the metal pipe. The capacitor is connected at point 3 of LT1360CN8 to the ground. After that, the peak detector is used to output the peak value of the input AC signal. The peak detector used is the simplest design which consists of two which are 100pF capacitor and BAT81 diode. The simulation of the circuit is successfully changing the AC signal to DC signal. But when applying the circuit to the real situation, the peak detector circuit was not successful to change the AC signal to DC signal and affecting the data recorded from sensor jig since it was manually taken. Since it was taken manually, human error exists and reduce the accuracy of the data taken and also affecting the accuracy of the image reconstruction. the result for simulation and real result is shown in**Error! Reference source not found.**.

Figure 3.11 Signal Conditioning Circuit
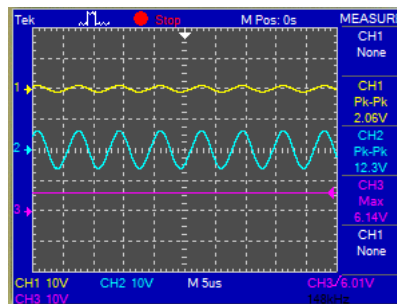
Figure 3.12 Simulation Result

Figure 3.13 Real Result

3.5 Image Reconstruction

Linear Back Projection Method (LBP) method was used in the project. It is used as the mathematical model in MATLAB software. The basic equation for LBP is shown in 2.8. The flow process of LBP is shown in Figure 3.14 .
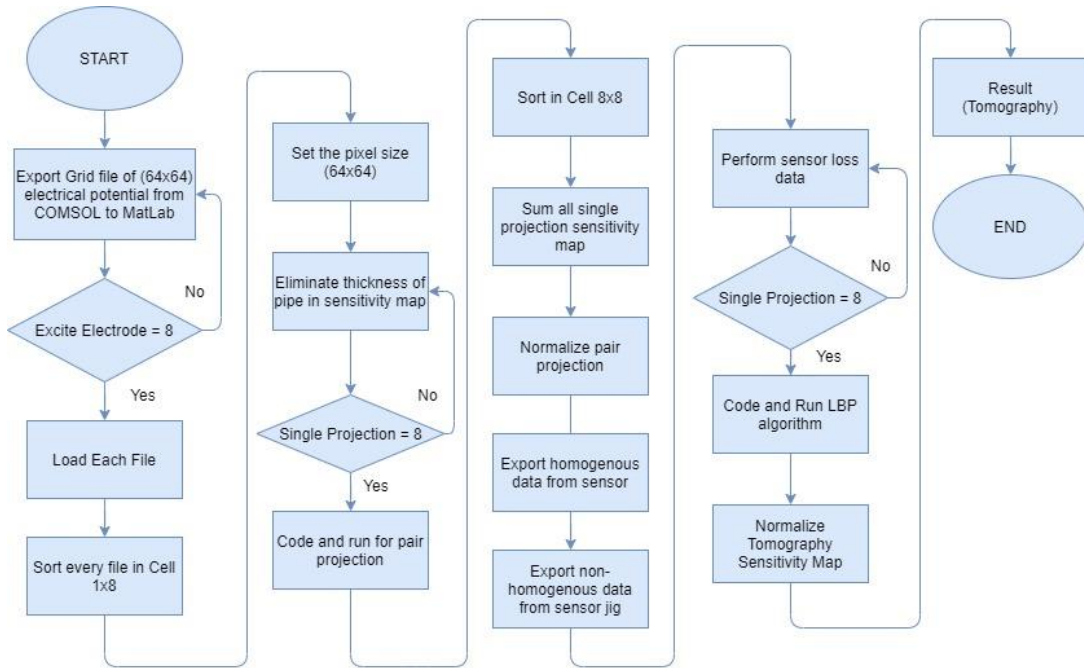

Figure 3.14 Flow chart of LBP method

The efficiency of the tomogram is then investigated using the multi scale structural similarity (MSSIM). The MSSIM is a method that compare between the resulting image and the reference image. The resulting of the MSSIM output index is from 0 to 1. The greater the MSSIM index value, the more accurate the image being reconstructed.

3.6 Sensitivity Map

The reconstruction method for ECT image can be done through several methods such iterative, and back projection. For every reconstruction method of ECT system, a sensitivity map is required for image reconstruction, since it serves as the base for combining individual pixels taken at various locations[18]. The sensitivity map, also known as the Jacobian matrix, is a matrix that shows the dynamic changes in capacitance between sensing electrodes when a voltage is applied. By solving the Poisson equation

of the electric field, sensitivity maps were constructed. In Finite Element Analysis (FEA), the permittivity distribution is assumed to be made up of multiple pixel elements, with each pixel's sensitivity coefficient expressed as

$$S_{ij(k)} = \left(\frac{C_{ij(k)} - C_{ij}^l}{C_{ij}^h - C_{ij}^l}\right)\left(\frac{1}{\varepsilon_h - \varepsilon_l}\right)\mu(k)$$

3.1

i = 1, 2, 3, . . . L − 1 j = i + 1, . . .L k= 1, 2, 3, . . . N

where,

$C_{ij(k)}$	capacitance of electrode pair i–j
C_{ij}^h and C_{ij}^l	capacitance of electrode pair at different permittivity, l and h
ε_h	high relative permittivity
ε_l	low relative permittivity
$\mu(k)$	ratio of maximum area to kth area.

The sensitivity map was created by using the simulation in the COMSOL Multiphysics software. The image reconstruction for the sensitivity map was created by exporting electrical potential data in 64x64 resolution and arranging the generated data in coordinate form. The data is normalised and imported into MATLAB, where it is plotted depending on their coordinates as shown in Table 3.3[18].

Table 3.3 Sensitivity map distribution when channel 1 as excitation electrode

j=1,i=2	j=1,i=3
j=1,i=4	j=1,i=5
j=1,i=6	j=1,i=7
j=1,i=8	
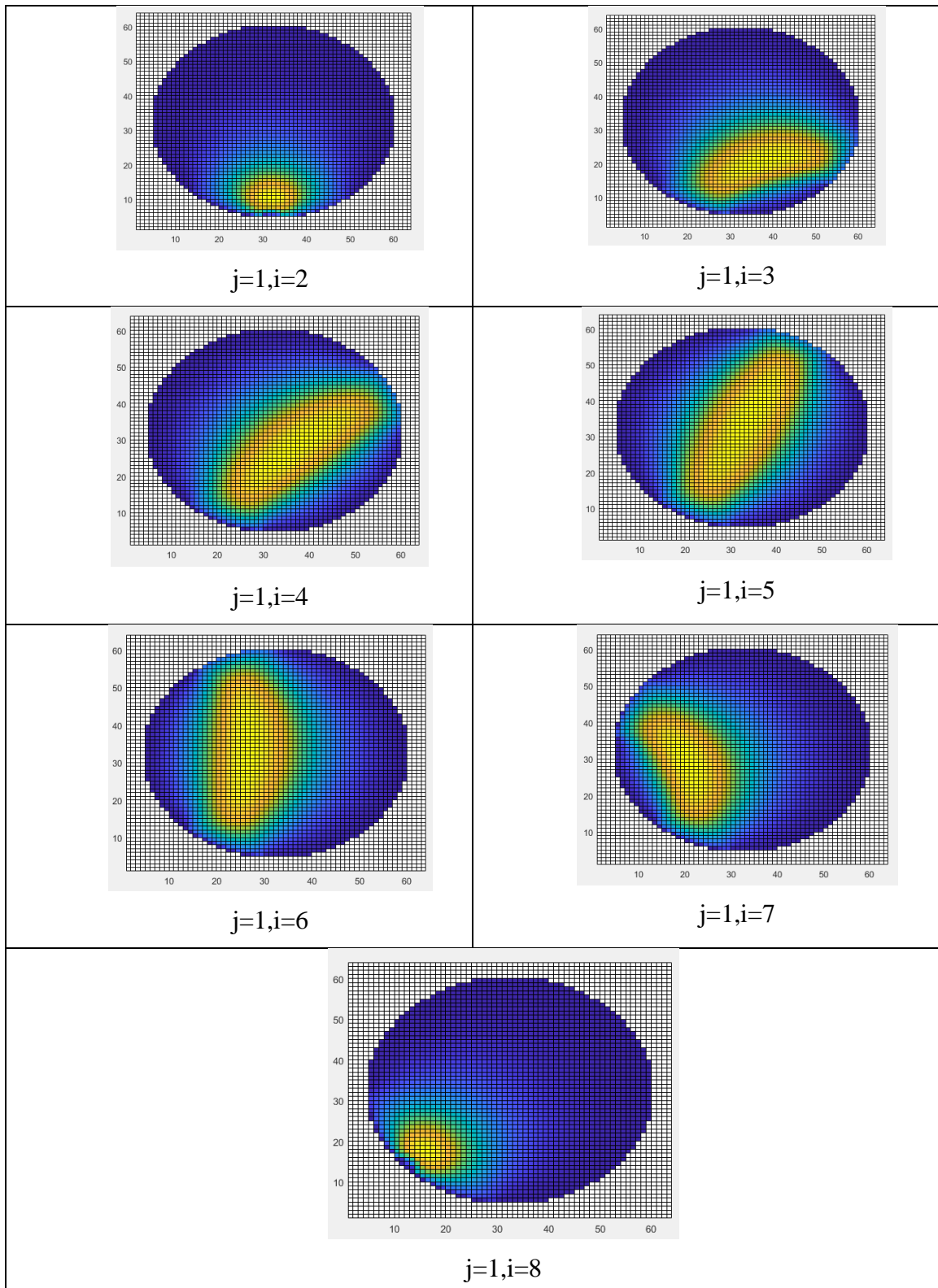
Based on the simulation, it is clear that the electrode arrangement has a significant impact on the production of sensitivity maps. By reconstructing the electrical potential data from the simulation, a sensitivity map was created. Different positions and distances

between electrode pairs have been shown to impact the electrode pair's projection path[18].

3.7   Summary

In this chapter, the method starts with design and development of the sensor jig. After that, the circuit for signal generator circuit and signal conditioning circuit were simulated using the Multisim software. The circuit was then constructed in real situation and 8 signal conditioning circuit was constructed. Then, the data from sensor jig is used for image reconstruction of LBP which was executed using MATLAB software.

CHAPTER 4

RESULTS AND DISCUSSION

4.1   Introduction

This chapter consists of the results and discussion of the invasive ECT system. The simulation for electrical measurement circuit was divided into two parts. The first part was obtained using the Multisim software to see the waveform for the results, the second part is to simulate using the hardware. Besides, the tomograms for each cases tested were also analysed.

4.2   Results

4.2.1   Result For Homogenous and Non-Homogenous

The measurement of the simulation which uses oil as the medium and PVC pipe as the phantom is conducted in this project. The data is collected from the metal pipe, and it is compared for homogenous and non-homogenous conditions. The 20mm PVC pipe is placed inside metal pipe and in front of electrode 7. By plotting the homogenous and non-homogenous of electrical potential between interaction electrode 1 (excitation electrode) and the other 7 electrodes (receiver), the distorted value approaching the obstacle is different in relative permittivity between the obstacle and oil. The position of the receiver when the electrode 7 as transmitter is shown in Figure 4.1 and the value electrical potential of both homogenous and non-homogenous is plotted into a graph that is shown in Figure 4.4. The changes of homogenous and non-homogenous can also be seen when putting the obstacle inside the sensor jig the difference in amplitude can be observe.
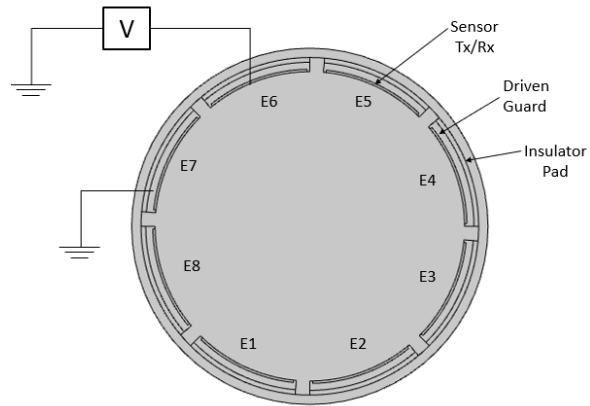
Figure 4.1 Position of the receiver and transmitter

Figure 4.2 Homogenous Amplitude
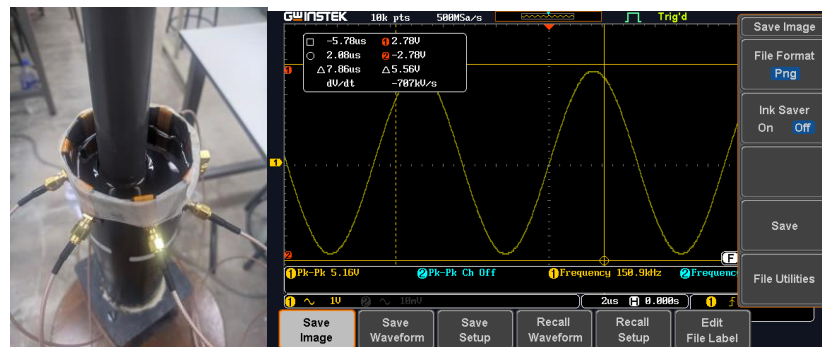
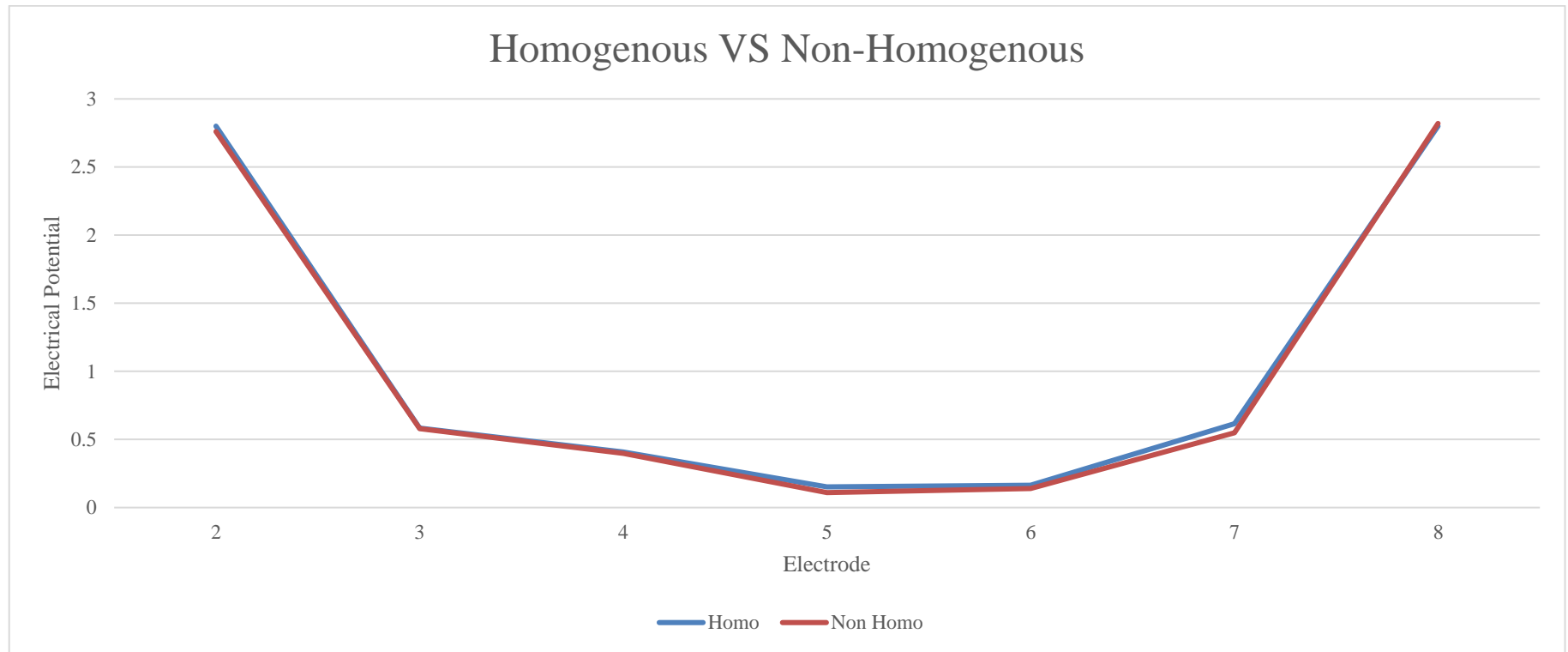Figure 4.3 Non-Homogenous amplitude changes

Figure 4.4 The comparison of the value electrical potential with homogenous and non-homogeneous.

It can be observed that the value of potential difference at E4, E5 E6, E7 and E8 is decreased. It is because of the presence of the PVC pipe was blocking the path of electrical field distribution from excited to electrode to the E4, E5 E6, E7 and E8 and it was reflected by the PVC pipe.

4.2.2 Adjacent and Opposite

When transmitting signal from 1 terminal. For this test, the transmitter from electrode 1, the adjacent is from electrode 2 while the opposite is from electrode 5. The further the distance from transmitter, the lower the electrical voltage potential value. It can be seen in the Figure 4.6 and Figure 4.7 below. It is proven that the adjacent receiver shows higher electrical potential voltage while the opposite is lower.
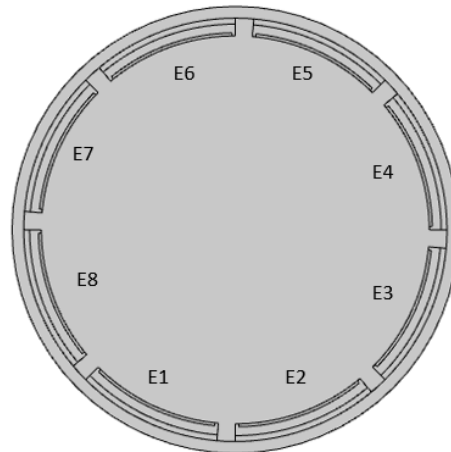
Figure 4.5 E1 as transmitter, E2 as adjacent receiver and E5 as opposite receiver
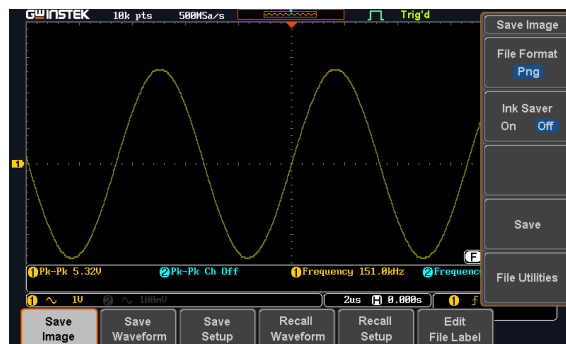
Figure 4.6 Adjacent Receiver E2
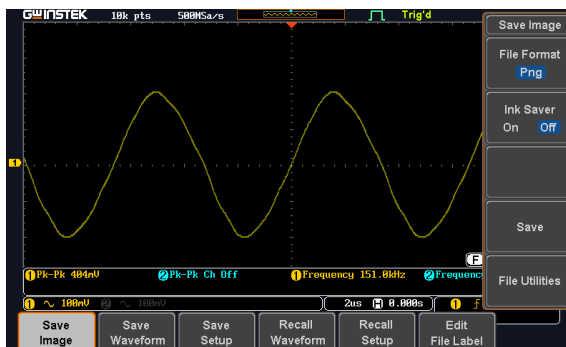

Figure 4.7 Opposite Receiver E5

4.2.3   Results for three conditions

After proving the homogenous and non-homogenous changes in relative permittivity of the subject conducted in the project, it is continued with three different conditions. By using the same procedure, the different conditions of the obstacle are measured. The three conditions of the obstacle are the size of the obstacle, the position of the obstacle and the number of the obstacle inside the sensor jig. Each condition is measured three times with different observation and the results are shown in Table 4.1, Table 4.2,and Table 4.3 .

First, Table 4.1 shows the result of the different sizes of obstacle placed in the middle of the sensor jig and was done with three different diameter of the obstacle that were 20mm, 25mm and 33mm. Next, Table 4.2 shows the result of three different positions of the air bubble which were placed at middle, right side and bottom left of the sensor jig. The experiment was completed using the 33mm obstacle.

Finally, Table 4.3 shows the result of different number of obstacles present inside the sensor jig which were one 20mm and 33mm obstacle, two 20mm obstacle and three 20mm obstacle. The values of electrical potential for all conditions were obtained and line graph was compared with homogenous that is shown in Figure 4.12, Figure 4.13, Figure 4.14, Figure 4.15, Figure 4.16, Figure 4.17, Figure 4.18, Figure 4.19, Figure 4.20.

Table 4.1 The effect of different obstacle size

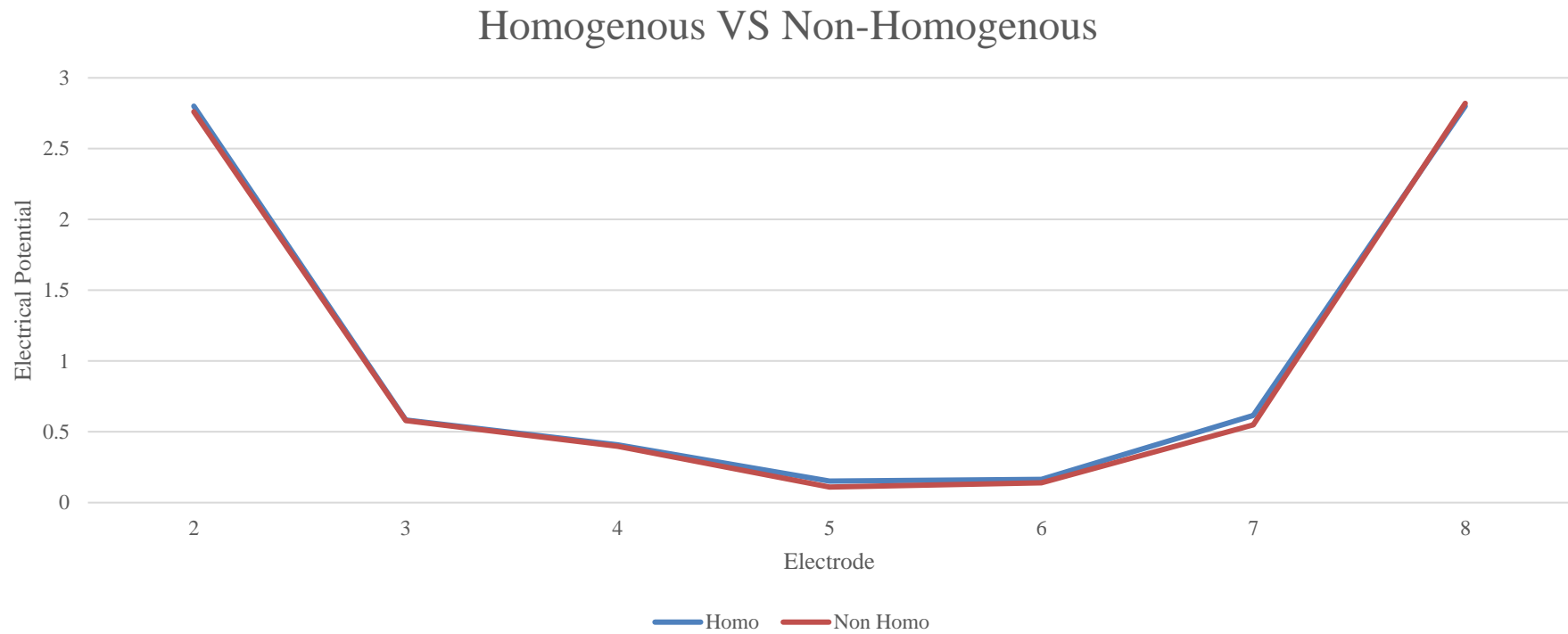| Phantom Size	Geometry	Reference Image
20mm		
25mm		
33mm		
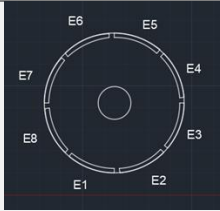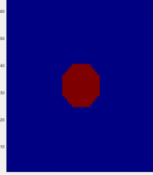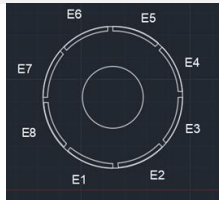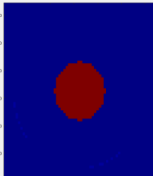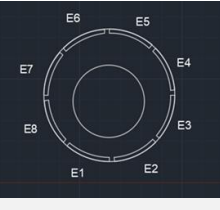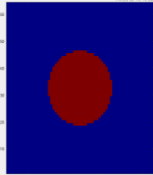
Figure 4.8 The line graph comparison of value electrical potential between homogenous and obstacle size 20mm

From Figure 4.8 , the electrical potential for E5, E6 and E7 were decreased compared to the homogenous.
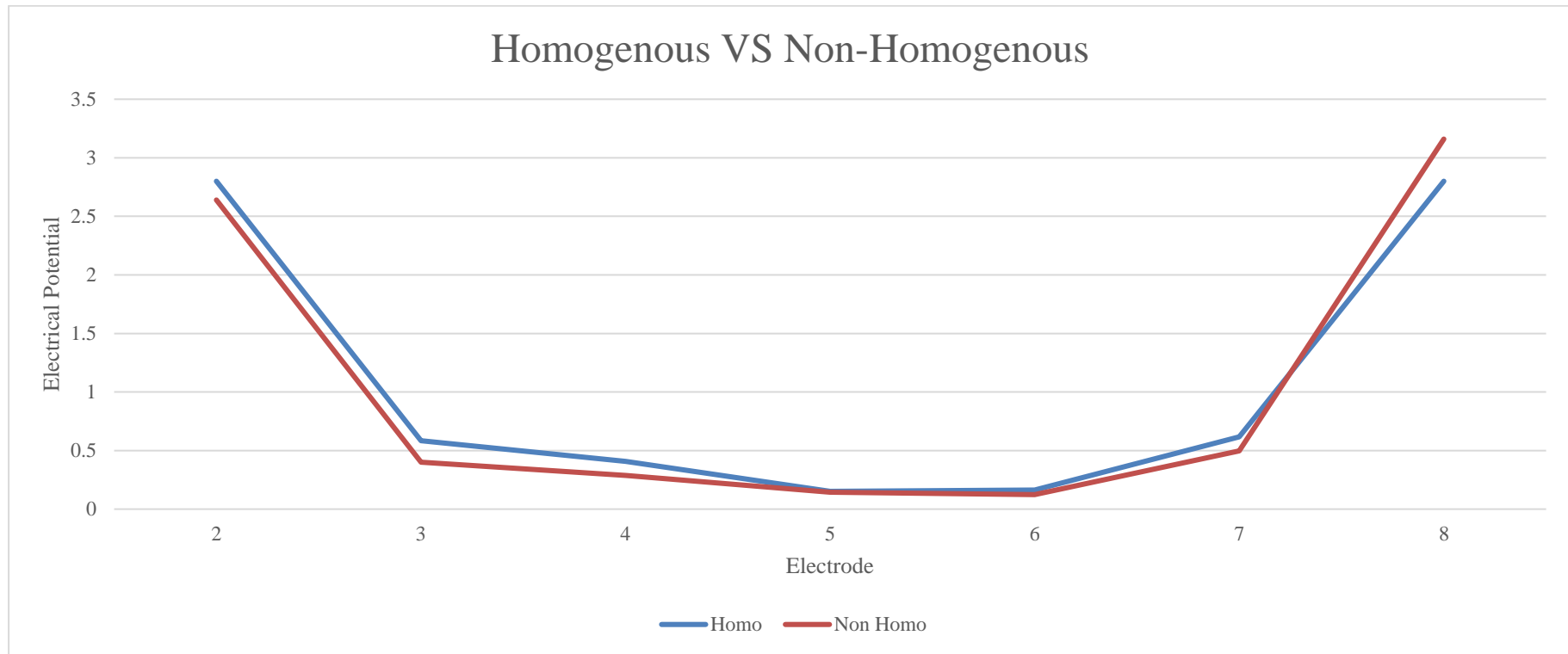
Figure 4.9 The line graph comparison of value electrical potential between homogenous and obstacle size 25mm

From Figure 4.9, the electrical potential for E2, E3, E4, E6, E7 were decreased and E8 was increased compared to the homogenous.
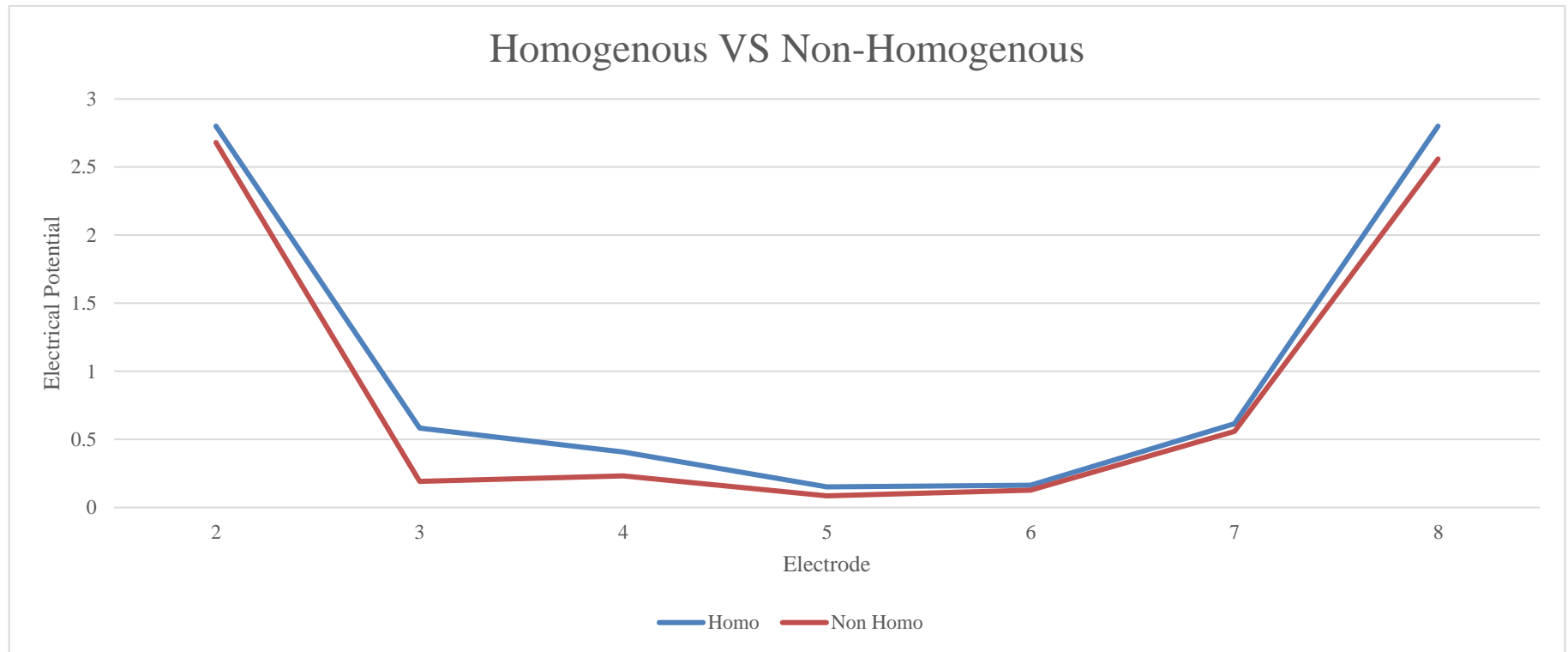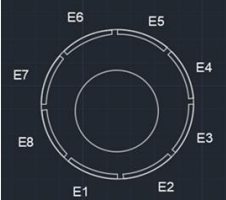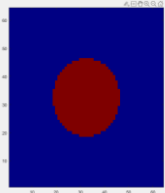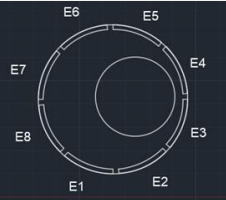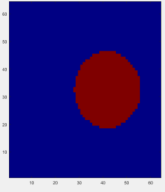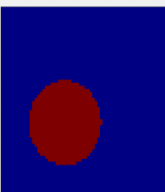
Figure 4.10 The line graph comparison of value electrical potential between homogenous and obstacle size 25mm

From Figure 4.10, the electrical potential for all the electrode were decreased compared to the homogenous.

Table 4.2 The effect of different obstacle positions

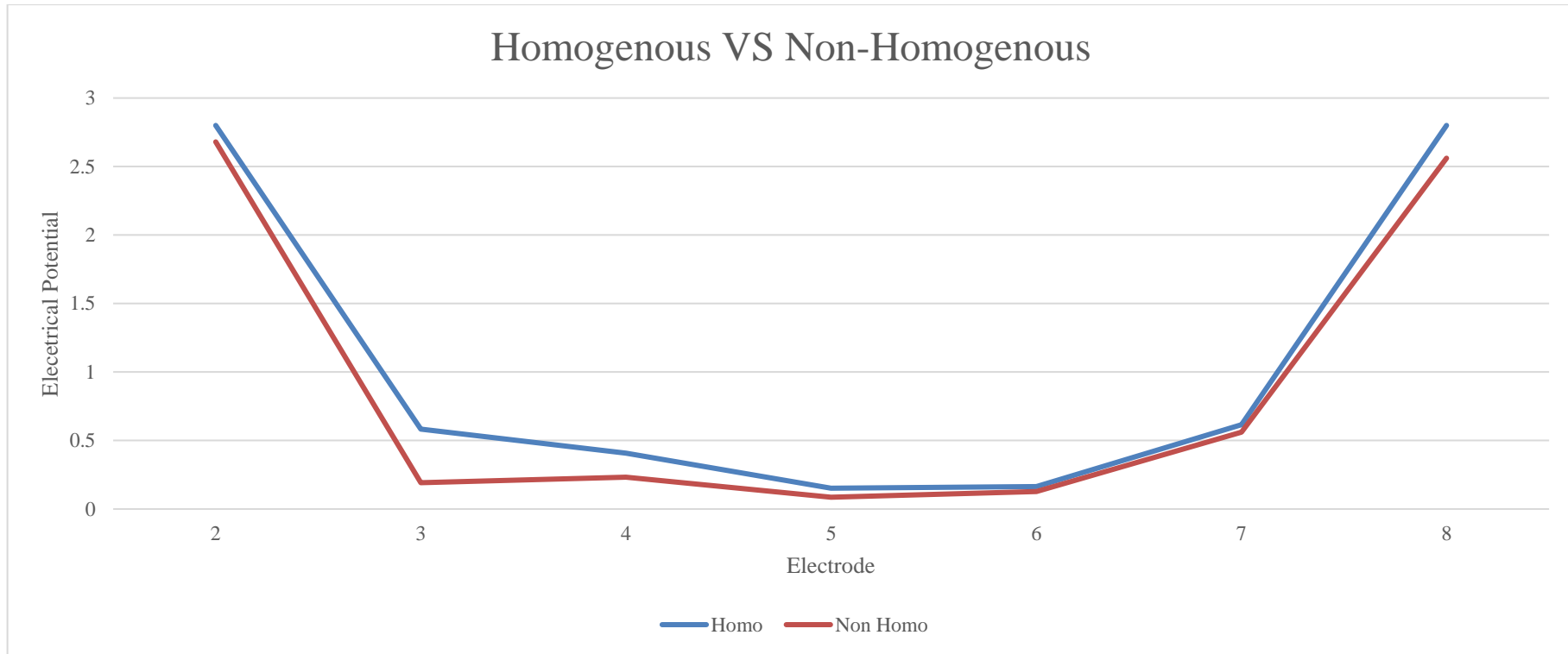| Phantom Position	Geometry	Reference Image
Middle		
Right Side		
Bottom Left		

Figure 4.11 The line graph comparison of value electrical potential between homogenous and obstacle size at middle

From Figure 4.11, the electrical potential for all electrodes were decreased compared to the homogenous.
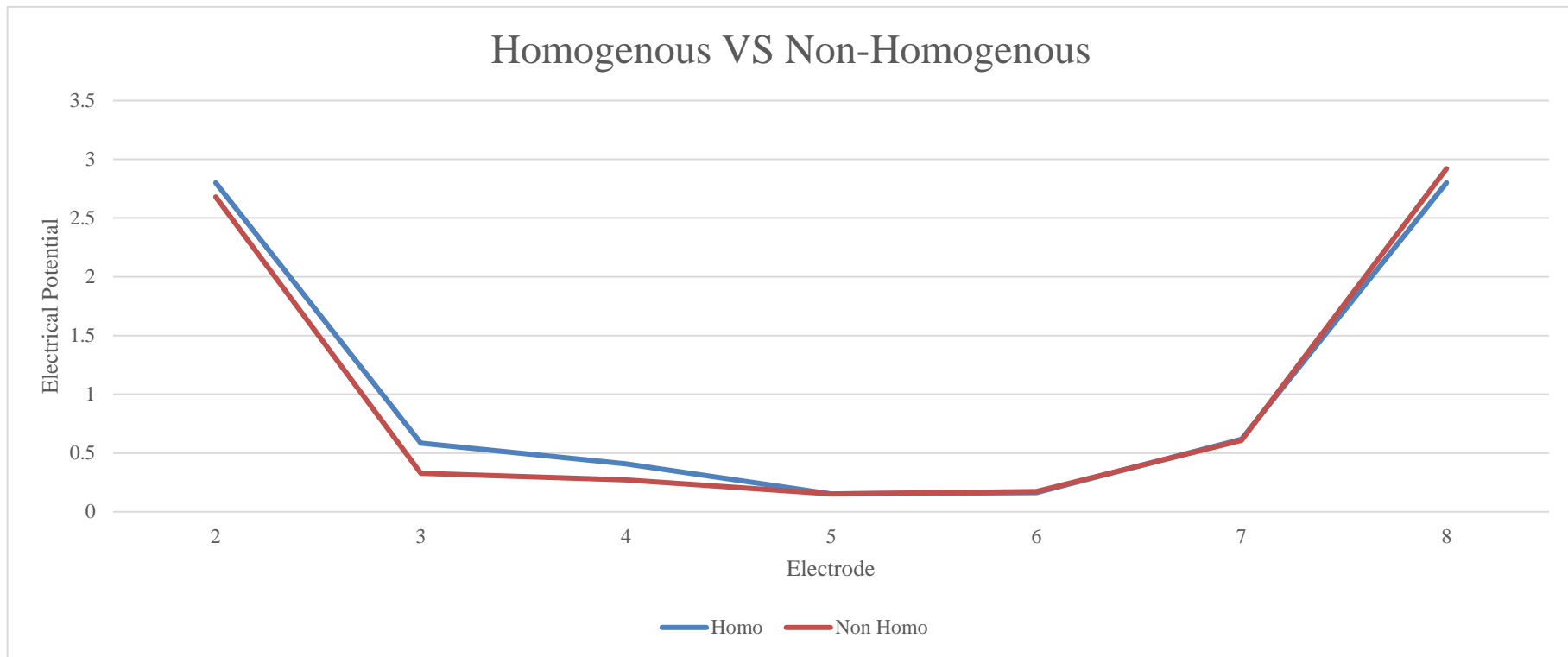
Figure 4.12 The line graph comparison of value electrical potential between homogenous and obstacle at right side

From Figure 4.12, the electrical potential for E2, E3, E4 and E7 were decreased while E8 has increased compared to the homogenous.

Figure 4.13 The line graph comparison of value electrical potential between homogenous and obstacle at bottom left

From Figure 4.13, the electrical potential for E3, E4, E7 and E8 were decreased while E2 has increased compared to the homogenous.
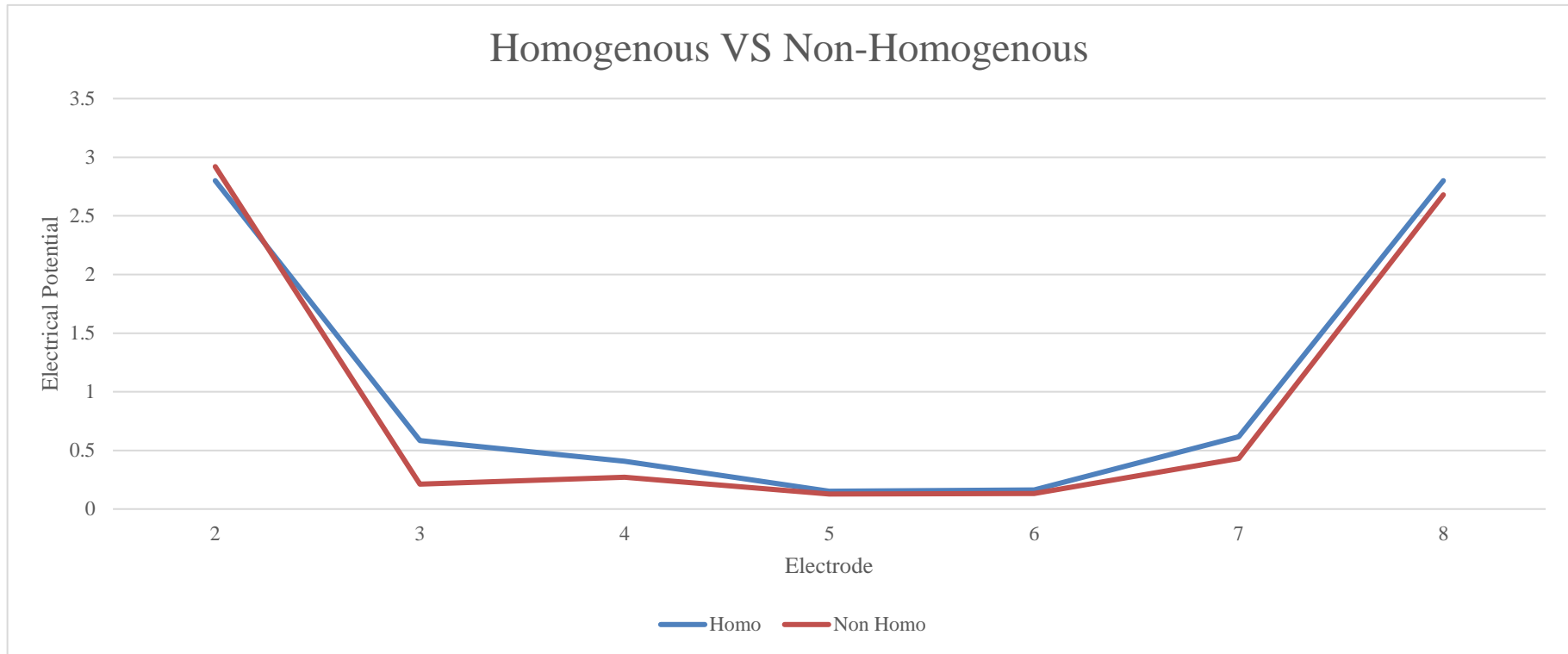
Table 4.3 The effect of multiple obstacles

Phantom	Geometry	Reference Image
33mm and 20mm		
Two 20mm		
Three 20mm		

Figure 4.14 The line graph comparison of value electrical potential between homogenous and 20mm obstale and 33mm obstacle

From Figure 4.14, the electrical potential for all the electrodes were decreased compared to the homogenous.
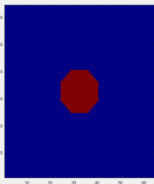
Figure 4.15 The line graph comparison of value electrical potential between homogenous and two 20mm obstacle

From Figure 4.15, the electrical potential for E2, E3, E4, E7 and E8 were decreased and E5 were slightly increased compared to the homogenous.
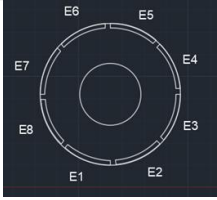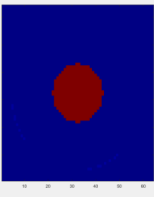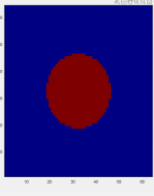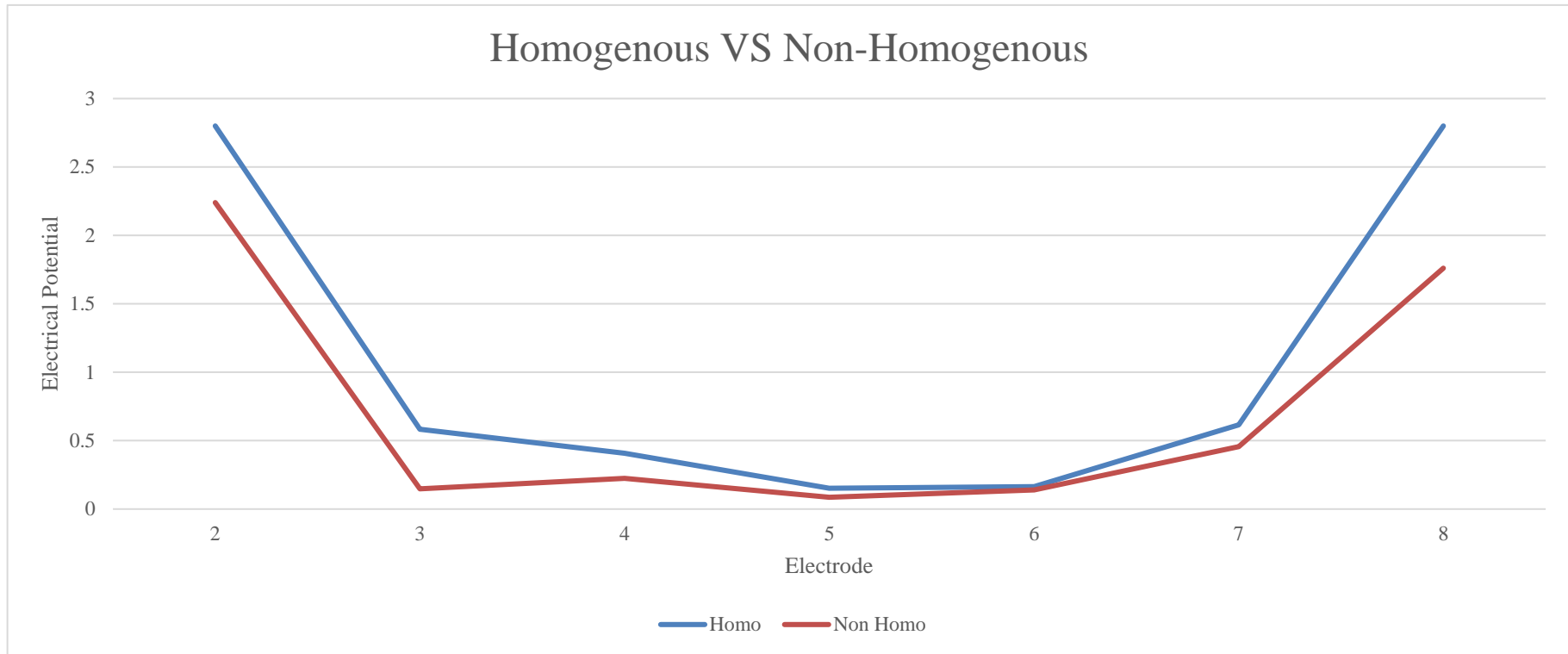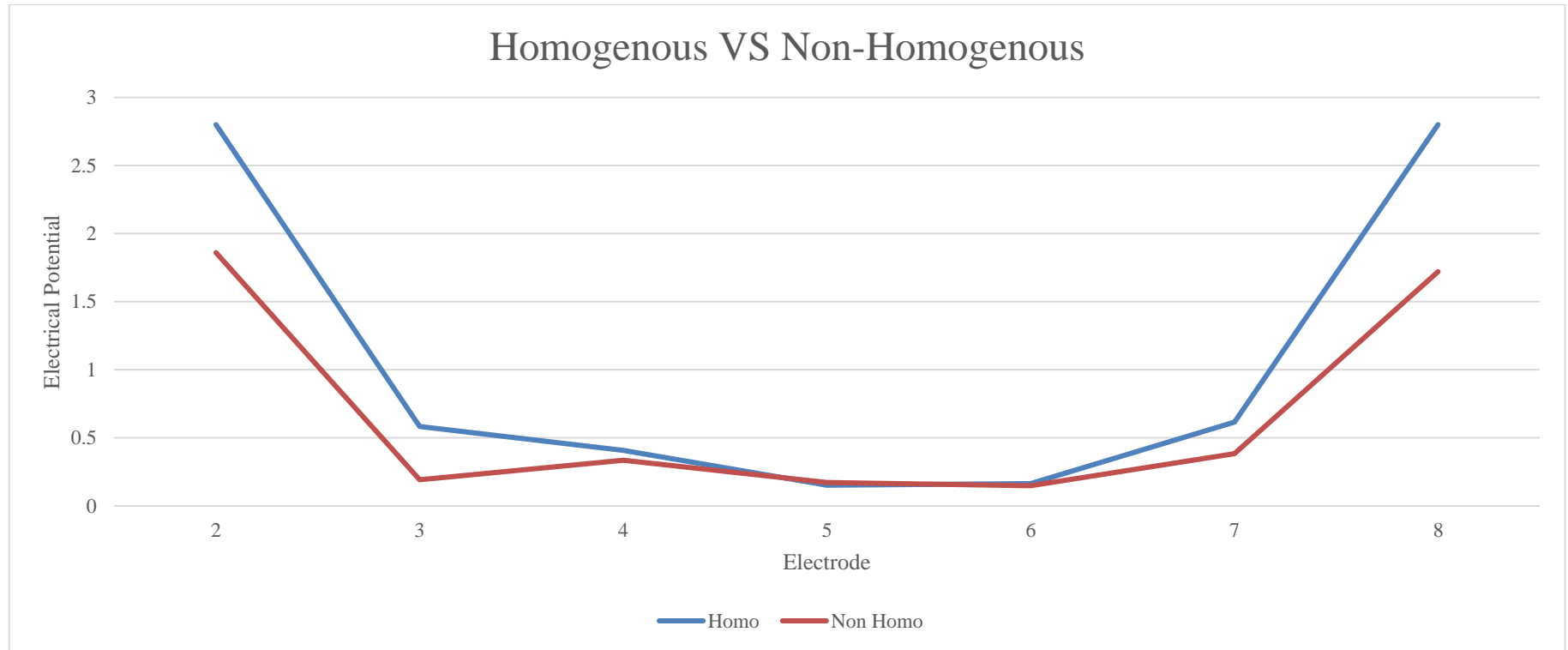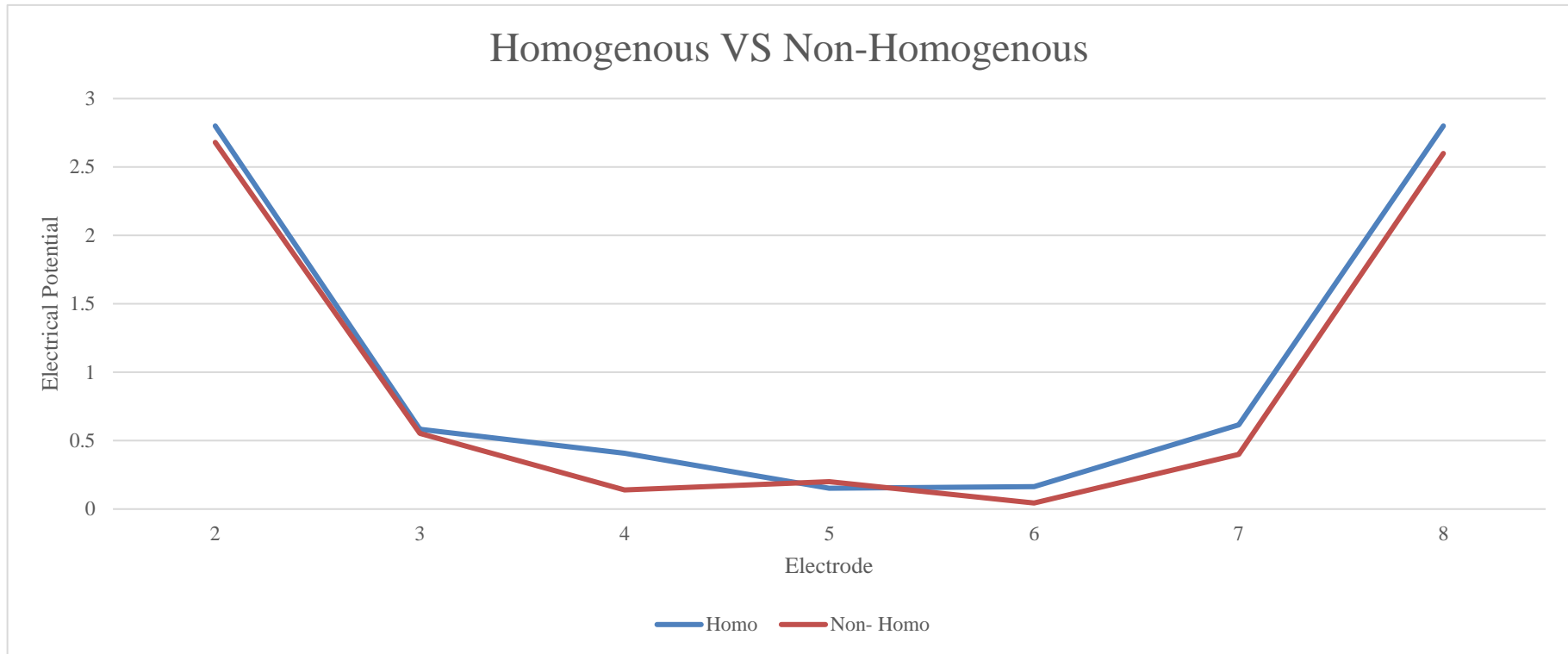
Figure 4.16 The line graph comparison of value electrical potential between homogenous and three 20mm obstacle

From Figure 4.16, the electrical potential for E2, E3, E4, E6, E7 and E8 were decreased while E5 has slightly increased compared to the homogenous.

From Table 4.1, the obstacle with the diameter of 20mm had less distortion compared to that with 25mm, while obstacle with 25mm had less distortion to the 33mm obstacle.

The changes in electrical potential between homogenous and non-homogenous can be seen from the line graph. There always appear the decrement of electrical potential at the receiver. It is caused by of the path of transmitter that projects the electric potential were blocked by the obstacle. Hence the reading of electrical potential at the receiver is decreased because of the blocked path.

It can be concluded that when the increment size and number of obstacles in the ECT would affect the increment in the number of the receivers with electrical potential loss.

4.2.4   Result For Image Reconstruction of Three Different Conditions

After getting the data for all three of the conditions from sensor jig, the project final step is to reconstruct the image. By using the MATLAB software, the LBP algorithm is used to generate the tomogram for all the conditions of the obstacle. the same condition that has been used in in part 4.2.2 were applied.

Table 4.4 shows the tomogram of the different obstacle sizes which were 20mm, 25mm and 33mm. Besides, Table 4.5 shows the tomogram of the different obstacle (33mm in diameter) positions which were at the middle, right side and bottom left, while Table 4.6 shows the tomograms of the different number of obstacle which were 20mm and 33mm, two 20mm and three 20mm obstacle. All of the results obtained contain the reference image, tomogram and MSSIM index.

Table 4.4 Image reconstruction for different obstacle size
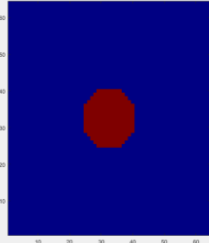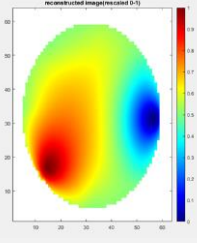
Phantom	Reference Image	Tomogram	MSSIM
20mm			0.0725
25mm			0.0985
33mm			0.1472
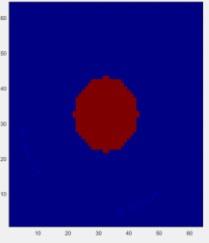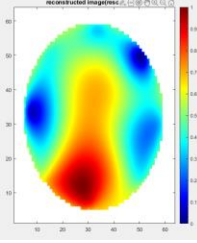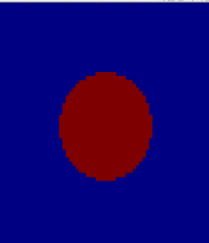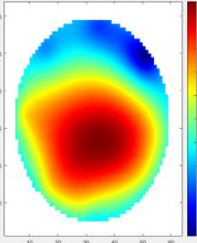
Table 4.5 Image reconstruction for different postion of obstacle

Phantom	Reference Image	Tomogram	MSSIM
Middle			0.1472
Right Sid			0.1323
Bottom Left			0.1240
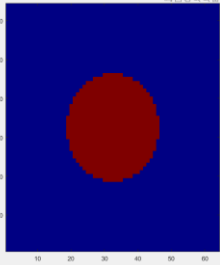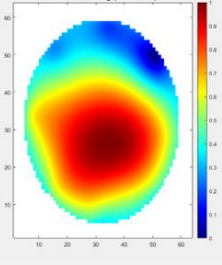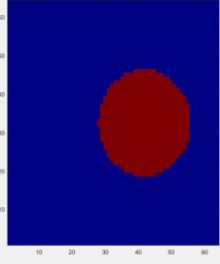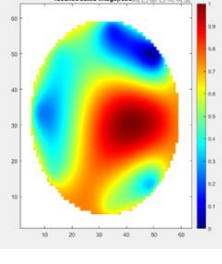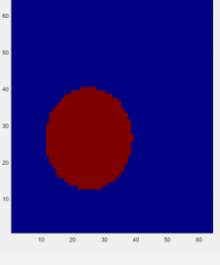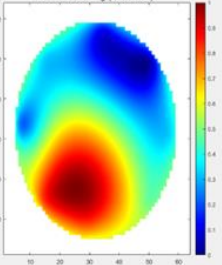
Table 4.6 Image reconstruction for multiple obstacle

Phantom	Reference Image	Tomogram	MSSIM
20mm and 33mm			0.1623
Two 20mm			0.0895
Three 33mm			0.1443
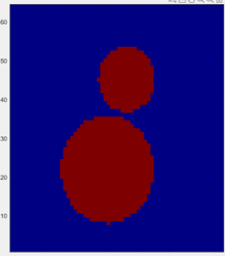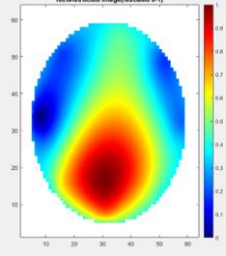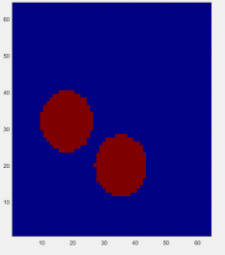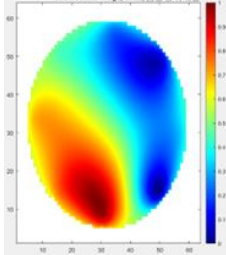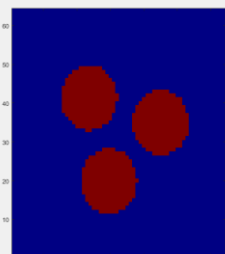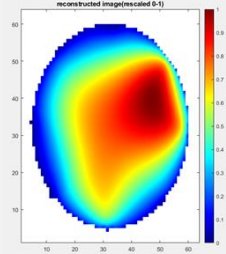
From Table 4.4, it can be seen that   20mm and 25mm tomogram is almost cannot be read or not identical to the reference image. This is because of the obstacle is to small and there exists the limitation of the sensor jig. The image that had been reconstructed by the LBP algorithm produce smearing effect and reduces the quality of the image. The MSSIM Index also show higher value when the obstacle is bigger. The bigger the obstacle present, the tomogram reconstructed also shown a better quality can be generated by the LBP.

Moreover, Table 4.5 has proven that LBP can also generate tomogram even with distinguish position. Bottom left has the lowest MSSIM index since the position is a little bit further from the electrode. Disadvantage of LBP is when the further the distance between the obstacle and sensor, the performance of the tomogram to capture the accurate position was also decreased.

Finally, the Table 4.6 were blurred with the increment of the obstacle due to the smearing effect. The increment of the obstacle rose the smearing effect in LBP algorithm, hence resulting the blurriness of tomogram.

4.3   Summary

For homogenous and non-homogenous condition, the difference can be seen from the electrical potential graph. The obstacle results in distorted value of the non-homogeneous. Moreover, when the different sizes and multiple obstacles would result in the increment of distortion on the electrical potential value.   In image reconstruction part using MATLAB, it shows that 20mm and 25mm obstacle and the two 20mm obstacle showed the lowest value of the MSSIM index. The circuit of signal conditioning is needed to be improved, since manually taken data from sensor jig can reduce the accuracy of the data, hence human error occurs.

CHAPTER 5

CONCLUSION

5.1   Conclusion

The objectives of the project were partially achieved. Based on the objective of the project, the design of the electrical measurement circuit of invasive ECT system including the signal generator and signal conditioning circuit is not fully achieved. All the circuit that been used in the project were all simulated using the NI Multisim software before testing in real situation. The signal conditioning circuit is not able to change the AC signal to DC signal. Hence, lowered the accuracy of the data obtained and the image that was reconstructed.

The sensor jig of the ECT was then developed based on invasive approach. Since oil and gas industry uses metal and steel pipe as conducting medium, the application of common ECT method is not suitable since the metal and steel pipe will act as electrical shield. Thus, the development of ECT invasive approach is another alternative to the common ECT. Besides, the first sensor was injected by 20V and 150kHz sine wave, then the other 7 will act as receiver. It will be repeated until all the sensor was excite. The electrical potential graph show decrement if obstacle is present inside the sensor jig.

After that, the testing of the ECT model was continued with three different conditions; different sizes, position and multiple obstacles. It can be seen that smaller size and a smaller number of obstacles resulted in lower distortion. When obstacle was present, the electrical potential graph will show changes. The tomogram showed good quality tomogram when the size of obstacle is bigger. The data obtained from sensor jig will then be use for image reconstruction using the MATLAB simulation. By using the LBP algorithm to recreate image to investigate the distribution component inside the sensor

jig. Disadvantage of LBP was if the distance between obstacle and the sensor is further, the performance of the tomogram to capture the exact position of the obstacle is lower. Another disadvantage is that it will creates blurry images which is also known as smearing effects. The increment number of obstacle in sensor jig rose the smearing effect in LBP algorithm, increasing the blurriness of tomogram. Overall, the LBP was able to produce a good tomography despite the smearing effect and lack of preciseness regarding obstacle position.

5.2   Problem Encounter

The main problem occur in this project was when designing the circuit. The simulation of the circuit was successful and it was expected that the user can get the desired result. When the circuit is implemented in the real situation which is connecting in breadboard, the result was differ and did not went well as planned. This problem has costed the data since it reduces the accuracy of the data. The data is taken manually and human error is present while taking the data.

To place the electrode inside the sensor jig is also troublesome. The sensor inside the sensor jig needed to be equally spaced. The problem can cause the reading of the data is not stable.

5.3   Future Recommendation

Through this project, several recommendations for future works are listed as follow:

I.   The number of electrodes can be increased so the reading inside sensor jig is improved.

II.   The sensor placement inside the sensor jig can be improved with permanent placement of the sensor.

III. The signal conditioning circuit can be redesigned to increase the accuracy of data taken.

REFERENCES

[1]   D. Yang, L. Liu, and W. Feng, "Experimental investigation of an internally circulating fluidized bed with 32-electrode electrical capacitance volume tomography," *Meas. J. Int. Meas. Confed.*, vol. 127, no. May, pp. 227–237, 2018, doi: 10.1016/j.measurement.2018.05.076.

[2]   M. S. Senen, E. J. Mohamad, H. L. M. Ameran, R. A. Rahim, O. F. Marwah, and S. Z. M. Muji, "Simulation analysis of dual excitations method for improving the sensitivity distribution of an Electrical Capacitance Tomography system," *Int. J. Integr. Eng.*, vol. 9, no. 1, pp. 10–15, 2017.

[3]   P. Ii, "Investigating the characteristics of varieties," 2020.

[4]   Ruzairi Abdul Rahim, "Electrical Capacitance Tomography: Principles, Techniques and Applications -," *Penerbit UTM Press*, 2011. .

[5]   Z. Li, Y. Chen, Y. Yang, C. Liu, M. Lucquiaud, and J. Jia, "Flow regime transition in countercurrent packed column monitored by ECT," *Chem. Eng. J.*, vol. 420, no. P1, p. 129841, 2021, doi: 10.1016/j.cej.2021.129841.

[6]   I. Saied and M. Meribout, "Electronic hardware design of electrical capacitance tomography systems," *Philos. Trans. R. Soc. A Math. Phys. Eng. Sci.*, vol. 374, no. 2070, 2016, doi: 10.1098/rsta.2015.0331.

[7]   N. Osman-Ali, J. Mohamad-Saleh, Z. Abdul-Aziz, and H. Talib, "Optimization of Electrical Capacitance Tomography sensor using design of experiment method," *J. Teknol. (Sciences Eng.*, vol. 55, no. SPECIAL EDITION2, pp. 87–99, 2011, doi: 10.11113/jt.v55.893.

[8]   K. Perera, C. Pradeep, S. Mylvaganam, and R. W. Time, "Imaging of oil-water flow patterns by Electrical Capacitance Tomography," *Flow Meas. Instrum.*, vol. 56, no. July, pp. 23–34, 2017, doi: 10.1016/j.flowmeasinst.2017.07.002.

[9]   N. Amizan *et al.*, "A Review on Electrical Capacitance Tomography Sensor Development," *J. Teknol.*, vol. 3, no. 73, pp. 35–41, 2015.

[10]   F. Wang, Q. Marashdeh, L. S. Fan, and W. Warsito, "Electrical capacitance volume tomography: Design and applications," *Sensors*, vol. 10, no. 3, pp. 1890–1917, 2010, doi: 10.3390/s100301890.

[11]   E. Johana, F. R. M. Yunus, R. A. Rahim, and C. K. Seong, "Hardware development of electrical capacitance tomography for imaging a mixture of water and oil," *J. Teknol. (Sciences Eng.*, vol. 54, pp. 425–442, 2011, doi: 10.11113/jt.v54.825.

[12] R. Omar, B. Hewakandamby, A. Azzi, and B. Azzopardi, "Fluid structure behaviour in gas-oil two-phase flow in a moderately large diameter vertical pipe," *Chem. Eng. Sci.*, vol. 187, pp. 377–390, 2018, doi: 10.1016/j.ces.2018.04.075.

[13] "PTL APPLICATION NOTE AN3 ENGINEERING DESIGN RULES FOR ECT SENSORS Issue 4 March 2001," no. 4, 2001.

[14] F. A. Phang, J. Pusppanathan, and R. A. Rahim, "Portable Electrical Capacitance Tomography Device for Teaching and Learning of Engineering Instrumentation in Electrical Engineering Laboratory," *Proc. - 2017 7th World Eng. Educ. Forum, WEEF 2017- Conjunction with 7th Reg. Conf. Eng. Educ. Res. High. Educ. 2017, RCEE RHEd 2017, 1st Int. STEAM Educ. Conf. STEAMEC 201*, pp. 400–404, 2018, doi: 10.1109/WEEF.2017.8467170.

[15] J. Lei and Q. B. Liu, "Reconstruction method with the learned regularizer for imaging problems in electrical capacitance tomography," *Appl. Soft Comput. J.*, vol. 89, p. 106126, 2020, doi: 10.1016/j.asoc.2020.106126.

[16] Y. Li and M. Soleimani, "Imaging conductive materials with high frequency electrical capacitance tomography," *Meas. J. Int. Meas. Confed.*, vol. 46, no. 9, pp. 3355–3361, 2013, doi: 10.1016/j.measurement.2013.05.020.

[17] H. Wang and W. Yang, "Application of electrical capacitance tomography in circulating fluidised beds – A review," *Appl. Therm. Eng.*, vol. 176, no. January, p. 115311, 2020, doi: 10.1016/j.applthermaleng.2020.115311.

[18] M. Ma and Y. Yang, *Lecture Notes in Electrical Engineering: Preface*, vol. 223 LNEE, no. VOL. 1. 2013.

[19] Q. Marashdeh, "Advances in Electrical Capacitance," *Work*, 2006.

[20] "Principles of Electrical Capacitance Tomography," 1980.

[21] A. A. Hamzah *et al.*, "Simulation studies on image reconstruction algorithm for portable electrical capacitance tomography," *Int. J. Integr. Eng.*, vol. 10, no. 8, pp. 107–111, 2018, doi: 10.30880/ijie.2018.10.08.016.

[22] L. Zhang and M. Zhang, "Image reconstruction of electrical capacitance tomography based on optimal simulated annealing algorithm using orthogonal test method," *Flow Meas. Instrum.*, vol. 80, no. March, p. 101996, 2021, doi: 10.1016/j.flowmeasinst.2021.101996.

[23] Z. Xia, Z. Cui, Y. Chen, Y. Hu, and H. Wang, "Generative adversarial networks for dual-modality electrical tomography in multi-phase flow measurement," *Meas. J. Int. Meas. Confed.*, vol. 173, no. September 2020, p. 108608, 2021, doi:

10.1016/j.measurement.2020.108608.

[24]   Pengra D., "The Oscilloscope and the Function Generator : Some introductory exercises," pp. 1–19, 2007.

[25]   M. J. Lee, "Signal Conditioning Circuit Design," p. 10, 2011.

APPENDIX A
CODING FOR CALCULATE SENSOR LOSS

```matlab
%%Clear work space
clear all;
%%Load the sensor reading for full oil(Homo) and with obstacle(Non-
Homo)
%%Make sure the sensor reading value are electrical potential
%%If have N electrodes make sure the table are NxN for both
load fulloil;
load obstacle;
%%Make a repsentation for fulloil and obstacle
A=fulloil;
B=obstacle;
%%Calculate sensor loss
SL=(A-B)./A;
```

```matlab
%%Clear workspace
clear all;
%%Load all single projection file(make sure save as .mat)
load E1;
load E2;
load E3;
load E4;
load E5;
load E6;
load E7;
load E8;

%%Load the sensor los
load SL;
%%Sort the file in cell 1xN
EachProj={E1 E2 E3 E4 E5 E6 E7 E8};
%%Set the number of electrode//Set the pixel
N=8
pixel=64;
r = pixel/2; % radius
%%Eliminate the thickness of pipe
for i=1:N
for x=1:pixel
for y=1:pixel
if sqrt((x-pixel/2)^2+(y-pixel/2)^2)>=r-9
%%-ve value means how much to reduce;
%%reduce pheripehry of the image by looiking from the
grid pixel
EachProj{i}(x,y)=NaN; % set color reduced to the same
color base
end
end
end
end
%%Pair projection N x N cells
for i=1:N
ei=EachProj{1,i};
for j=1:N
ej=EachProj{1,j};
68
m= ei.*ej;
Epair{i,j}=m;
end
end
%Loop weighted balance map/ total map
W = EachProj{1};
for i=2:12
W = W + EachProj{i};
end
%Normalization of pair projections
for i=1:12
for j=1:12
norm = Epair{i,j}./W;
NormEpair{i,j}= norm;
end
end
```

```matlab
%LBP formula
DispMap= zeros(pixel);
for Tx=1:N
for Rx=1:N
DispMap= DispMap + (SL(Rx,Tx)*NormEpair{Rx,Tx});
end
end
%%-------Fixed scale 0 to 1------
normDispMap=DispMap; % rename display image
a = min(normDispMap(:));
b = max(normDispMap(:));
for Tx = 1:pixel;
for Rx = 1:pixel;
normDispMap(Tx,Rx) = ((normDispMap(Tx,Rx)-a)./ (b-a))*1;
%%Eliminate NaN value at norm DispMap ; if not matlab cant plot
img
e=normDispMap(Tx,Rx);
d=isnan(e);
e(d)=NaN;
normDispMap(Tx,Rx)=e;
end
end
%Displaying map
subplot(1,2,1);
pcolor(normDispMap(1:pixel,1:pixel))
imageCenter=[72.5,72.5];
title('reconstructed image(rescaled 0-1)');
shading interp; % To hide the grid line from pcolor
69
colormap (jet) % Change color map to jet colour
colorbar % Display colorbar at RHS
subplot(1,2,2);
imagesc(normDispMap(1:pixel,1:pixel))
set(gca, 'YDir', 'normal')
```

LINEAR TECHNOLOGY

LT1360
50MHz, 800V/μs Op Amp

FEATURES

- **50MHz Gain Bandwidth**
- **800V/μs Slew Rate**
- **5mA Maximum Supply Current**
- $9nV/\sqrt{Hz}$ Input Noise Voltage
- Unity-Gain Stable
- C-Load™ Op Amp Drives All Capacitive Loads
- 1mV Maximum Input Offset Voltage
- 1μA Maximum Input Bias Current
- 250nA Maximum Input Offset Current
- ±13V Minimum Output Swing into 500Ω
- ±3.2V Minimum Output Swing into 150Ω
- 4.5V/mV Minimum DC Gain, R_L=1k
- 60ns Settling Time to 0.1%, 10V Step
- 0.2% Differential Gain, A_V=2, R_L=150Ω
- 0.3° Differential Phase, A_V=2, R_L=150Ω
- Specified at ±2.5V, ±5V, and ±15V

APPLICATIONS

- Wideband Amplifiers
- Buffers
- Active Filters
- Video and RF Amplification
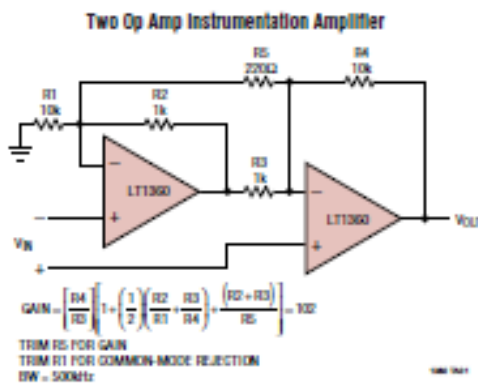- Cable Drivers
- Data Acquisition Systems

DESCRIPTION

The LT1360 is a high speed, very high slew rate operational amplifier with excellent DC performance. The LT1360 features reduced supply current, lower input offset voltage, lower input bias current and higher DC gain than devices with comparable bandwidth. The circuit topology is a voltage feedback amplifier with the slewing characteristics of a current feedback amplifier. The amplifier is a single gain stage with outstanding settling characteristics which makes the circuit an ideal choice for data acquisition systems. The output drives a 500Ω load to ±13V with ±15V supplies and a 150Ω load to ±3.2V on ±5V supplies. The amplifier is also capable of driving any capacitive load which makes it useful in buffer or cable driver applications.

The LT1360 is a member of a family of fast, high performance amplifiers using this unique topology and employing Linear Technology Corporation's advanced bipolar complementary processing. For dual and quad amplifier versions of the LT1360 see the LT1361/LT1362 data sheet. For 70MHz amplifiers with 6mA of supply current per amplifier see the LT1363 and LT1364/LT1365 data sheets. For lower supply current amplifiers with bandwidths of 12MHz and 25MHz see the LT1354 through LT1359 data sheets. Singles, duals and quads of each amplifier are available.

LT, LTC and LT are registered trademarks of Linear Technology Corporation.
C-Load is a trademark of Linear Technology Corporation.

TYPICAL APPLICATION

Two Op Amp Instrumentation Amplifier

$$GAIN = \left[\frac{R4}{R3}\right]\left[1+\left(\frac{1}{2}\right)\left(\frac{R2}{R1}+\frac{R3}{R4}\right)+\frac{(R2+R3)}{R5}\right] = 102$$

TRIM R5 FOR GAIN
TRIM R1 FOR COMMON-MODE REJECTION
BW = 500kHz

A_V = –1 Large-Signal Response
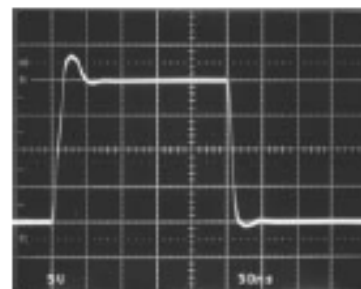
absolute maximum ratings over operating free-air temperature range (unless otherwise noted)[†]

Supply voltage, V_{CC+} (see Note 1) .... 22 V
Supply voltage, V_{CC-} .... −22 V
Differential input voltage, V_{ID} (see Note 2) .... ±44 V
Input voltage range, V_I (any input) .... V_{CC+} to V_{CC-} − 0.3 V
Input current, I_I (each input) .... ±1 mA
Output current, I_O .... ±80 mA
Total current into V_{CC+} .... 80 mA
Total current out of V_{CC-} .... 80 mA
Duration of short-circuit current at (or below) 25°C (see Note 3) .... unlimited
Package thermal impedance, θ_{JA} (see Notes 4 and 5): D package .... 97.1°C/W
    DW package ..... 57.3°C/W
    N package .... 79.7°C/W
    P package .... 84.6°C/W
    PW package ..... 108.4°C/W
Package thermal impedance, θ_{JC} (see Notes 4 and 5): FK package .... 5.6°C/W
    J package .... 15.1°C/W
    JG package ...... 14.5°C/W
    U package .... 14.7°C/W
Operating free-air temperature range, T_A: C suffix .... 0°C to 70°C
    I suffix .... −40°C to 105°C
    M suffix .... −55°C to 125°C
Storage temperature range .... −65°C to 150°C
Case temperature for 60 seconds: FK package .... 260°C
Lead temperature 1,6 mm (1/16 inch) from case for 10 seconds: D, DW, N, P, or PW package ..... 260°C
Lead temperature 1,6 mm (1/16 inch) from case for 60 seconds: J or JG package .... 300°C

[†] Stresses beyond those listed under "absolute maximum ratings" may cause permanent damage to the device. These are stress ratings only, and functional operation of the device at these or any other conditions beyond those indicated under "recommended operating conditions" is not implied. Exposure to absolute-maximum-rated conditions for extended periods may affect device reliability.

NOTES:
1. All voltage values, except differential voltages, are with respect to the midpoint between V_{CC+} and V_{CC-}.
2. Differential voltages are at IN+ with respect to IN−. Excessive current flows, if input, are brought below V_{CC-} − 0.3 V.
3. The output may be shorted to either supply. Temperature and/or supply voltages must be limited to ensure that the maximum dissipation rating is not exceeded.
4. Maximum power dissipation is a function of T_J(max), θ_{JA}, and T_A. The maximum allowable power dissipation at any allowable ambient temperature is $P_D = (T_J(max) − T_A)/\theta_{JA}$. Operating at the absolute maximum T_J of 150°C can affect reliability.
5. The package thermal impedance is calculated in accordance with JESD 51-7 (plastic) or MIL-STD-883 Method 1012 (ceramic).

recommended operating conditions

		C SUFFIX MIN	C SUFFIX MAX	I SUFFIX MIN	I SUFFIX MAX	M SUFFIX MIN	M SUFFIX MAX	UNIT
Supply voltage, $V_{CC\pm}$		±2	±22	±2	±22	±2	±22	V
Common-mode input voltage, V_{IC}	$V_{CC} = 5$ V	0	2.9	0	2.7	0	2.7	V
	$V_{CC\pm} = ±15$ V	−15	12.9	−15	12.7	−15	12.7	
Operating free-air temperature, T_A		0	70	−40	105	−55	125	°C